International Journal of Disaster Risk Reduction 112 (2024) 104757

Contents lists available at ScienceDirect

International Journal of Disaster Risk Reduction

journal homepage: www.elsevier.com/locate/ijdrr

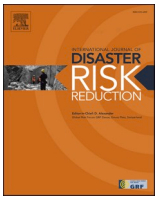

# Empirical seismic fragility of masonry buildings in historical centres accounting for structural interventions

Luca Sbrogiò, Ylenia Saretta *, Maria Rosa Valluzzi

*DBC - Department of Cultural Heritage, University of Padova, Piazza Capitaniato 7, 35139, Padova, Italy*

ARTICLE INFO

*Keywords:*
2016 central Italy earthquake
PGA and macroseismic intensity
Seismic damage
On-site surveys
Building inventory
Taxonomic system
Interventions on masonry buildings
Historical centres

ABSTRACT

Fragility models are widely employed to forecast seismic damage in built environments. However, the actual conditions of buildings, depending on their construction systems and transformations, are crucial for model reliability, especially in historical centres.

In this paper, an empirical fragility model for residential masonry buildings from data collected within 19 historical centres struck by the 2016 Central Italy earthquake is proposed. The dataset includes both traditional unreinforced and hybrid buildings, where reinforced concrete elements were applied in the 1980s according to seismic reinforcement prescriptions for existing structures.

This study acknowledges the impact of such structural modifications on the seismic performance of buildings, which can alter their vulnerability classification either improving or worsening it. The intensity measure for the fragility functions is the peak ground acceleration obtained from actual records through interpolation for each centre. Damage data and vulnerability assessment of 2134 traditional and hybrid structural units are conducted in the framework of the European Macroseismic Scale (EMS-98). The fragility functions are plotted for both structural types and EMS-98 vulnerability classes, also considering the contribution of structural interventions, and then compared to literature empirical models. Hybrid buildings achieve a behaviour similar to traditional buildings when floors are strengthened but walls are not. However, when both masonry walls and floors are strengthened, their performance significantly improved, approaching that of modern clay block buildings with rigid floors. Compared to literature models, the proposed one showed good compatibility for the most vulnerable buildings, whereas less vulnerable ones appeared even stronger thanks to interventions.

## 1. Introduction

Buildings in historical centres are stratifications of many phases, which have occurred over time due to recurring transformations since their foundation, often dating back to the Middle Ages. Any formal, geometrical and structural change is connected to variations in function, construction techniques, and ownership, and distorts the original layout. Poor construction techniques and locally available materials, such as stone or solid bricks for masonry walls and timber beams for floors and roofs [1,2], cannot ensure the 'box-like behaviour' of such traditional buildings [3] as the collaboration among structural elements is limited by interlocking and simple support. Therefore, in seismic areas, pre-modern masons devised aseismic devices compatible with the masonry structures such as buttresses, reinforcing arches and tie rods [4,5].

However, during the 20th century, reinforced concrete (r.c.) usage was promoted in building repairing and reinforcing practice,

* Corresponding author.
*E-mail addresses:* luca.sbrogio@unipd.it (L. Sbrogiò), ylenia.saretta@unipd.it (Y. Saretta), mariarosa.valluzzi@unipd.it (M.R. Valluzzi).

https://doi.org/10.1016/j.ijdrr.2024.104757
Received 31 July 2024; Accepted 11 August 2024
Available online 13 August 2024

even in ancient masonry buildings in historical centres. Reinforcement theoretically targeted the 'box-like behaviour' of a building during an earthquake, through the strengthening of masonry walls (e.g., grout injections, r.c. jacketing, reinforced stitching), the stiffening or replacement of floors and the improvement of connections either among the bearing walls or among walls and diaphragms (ring beams). Although only the holistic usage of all these techniques would have obtained a proper reinforcement, singular application, and generally to floors, was much more common and without checking for compatibility with unreinforced parts [6,7]. In both cases, traditional buildings were completely altered in their material composition and in their load-bearing system, and 'hybrid' structures, whose seismic behaviour is characteristic of neither masonry nor r.c. buildings, were obtained [8].

The earthquakes that have occurred in Italy since the end of the last century tested on a real scale the behaviour of such hybrid buildings and often revealed fragile performances: in case of pervasive and holistic actions, the structural behaviour was satisfactory [9], but where partial strengthening had been carried out extensive failures were observed [10]. In Italy, hybrid buildings in historical centres are widespread owing to the considerable extent of the seismic areas; hence, a systematization and evaluation of their seismic performance is needed, in order to improve the strategies for seismic risk mitigation.

Fragility functions are a valuable tool in risk assessment procedures, as they provide a concise representation of how structures respond to hazards, including earthquakes [11,12]. In this framework, the definition of fragility functions for historical centres can support the seismic risk assessment of such a high cultural value context, which needs to be conserved for and shared with future generations [13]. This task may be challenging owing to the presence of both traditional and hybrid buildings, which define distinct structural types. As deeply discussed in Section 2, existing fragility models for the Italian context do not specifically address the contribution of strengthening on the seismic performance of traditional buildings, as they focus on the actual configuration of buildings, regardless of transformations.

This research explores the behaviour of traditional and hybrid buildings within Italian historical centres struck by the 2016 Central Italy earthquake in terms of empirical fragility functions, by considering structural types and vulnerability classes compatible with the European Macroseismic Scale (EMS-98, [14,15]), that are assessed through a purposely developed procedure [16,17]. The result will be helpful for supporting the seismic risk reduction policies in historical centres in order to avoid, firstly, the loss of human lives, and then, of historical buildings and their cultural value.

## 2. Fragility functions

As far earthquakes are concerned, given an intensity measure (IM) of the seismic event, fragility functions express the probability of reaching or exceeding a damage measure (DM) for a group of buildings whose either the vulnerability level or structural features are the same. A DM represents a predetermined limit state of a building's response to the external load assumed as IM [18]. Continuous engineering parameters are preferable as IMs, such as peak ground acceleration (PGA), velocity (PGV) or displacement (PGD). Although PGV and PGD are better related to observed damage [19], PGA is commonly assumed in engineering practice and research studies, and it will be also used in this work. The probability $P$ that the damage ($d_k$) experienced by a group of buildings reaches or exceeds a DM, i.e., the i-th damage grade ($D_{ki}$) associated to the j-th PGA value, is generally expressed through a lognormal cumulative distribution [20] that is defined by two parameters: $\theta_{Dki}$, the median value of the IM which determines a damage at least equal to the DM considered, and $\beta$, the standard deviation which quantifies the uncertainty of the distribution [21], as per Eq. (1), where $\Phi[.]$ is the standard error function.

$$P\left(d_k \geq D_{ki} \middle| PGA_j\right) = \phi\left[\frac{ln\left(\frac{PGA_j}{\theta_{D_{ki}}}\right)}{\beta}\right] \tag{1}$$

As $\theta_{Dki}$ and $\beta$ are the unknown parameters in Eq. (1), they can be found by means of either maximum likelihood estimation (MLE), which obtains the values that have the highest probability to generate the observations, or least squares method (LSM), which minimizes the difference between observations and estimates. In the former case, the results are closer to the actual values, in the latter they are more adherent to the sample, although more approximate [22].

Fragility models are generally obtained for groups of structures with similar features (structural types), which account for their intrinsic variability (e.g., materials, details, geometry), and they can be categorized depending on the approaches chosen to develop them as:

1. Empirical fragility functions, which are constructed from data collected after an earthquake. Initially, the distribution of DMs as a function of the IM, conditioned to structural characteristics (damage probability matrices, DPM [23]), are obtained, then the fragility curves are derived through statistical regression analyses [19,24].
2. Mechanical fragility functions, which are generated by using sets of 'archetype' buildings and leverage various analytical approaches to obtain the DM, such as kinematic [25,26], nonlinear static [25,27–29], or nonlinear dynamic analyses [11,30–32]; simplified models can be used as well [33–37].
3. Expert elicitation curves, from the expert opinion of professionals in the field, who provide their insights into the vulnerability of structures, i.e., at which IM a certain DM is met [11,18,32,38–40]. This method was used for the completion of the EMS-98 model [41].
4. Hybrid methods, which combine multiple approaches, e.g., observed structural types analysed through a mechanical approach [42,43].

**Table 1**
Overview of empirical and expert elicitation fragility curves for residential buildings for Italian earthquakes ('r.c.' stands for 'reinforced concrete', RB/TR stands for ring beams and/or tie rods).

| Reference | Structure | Earthquake (*) | Survey | Fitting procedure | Grouping criteria | Interventions |
|---|---|---|---|---|---|---|
| De Luca et al. [57] | r.c. | 11 | EEFIT | Linear regression | – | – |
| Del Gaudio et al. [22] | r.c. | 8 | AeDES | MLE | no. of floors | – |
| Del Gaudio et al. [58] | r.c. | 1; 2; 3; 4; 5; 6; 7; 8; 9 | AeDES | MLE | r.c. design + no. of floors | – |
| Ioannou et al. [55] | masonry, r.c. | 9 | AeDES | Generalised Linear Model | AeDES structural types; year built | – |
| Lagomarsino et al. [40] (**) | masonry | 2; 8 | AeDES | – | vertical structure + year built + no. of floors; EMS-98 vulnerability classes | – |
| Masi et al. [11] (**) | masonry, r.c. | 1; 2; 3; 4; 5; 6; 7; 8; 9 | AeDES | – | vertical structure + year built + no. of floors; EMS-98 vulnerability classes | Improvement of ductility |
| Menichini et al. [59] | masonry | 10 | AeDES | MLE | EMS-98 structural types | – |
| Miano et al. [47] | masonry | 11 | Satellite images | – | no. of floors + presence TR and TB | RB/TR |
| Rosti et al. [60] | masonry, r.c. | 2; 8 | AeDES | LSM | EMS-98 vulnerability classes + no. of floors; AeDES structural types | RB/TR |
| Rosti et al. [24] | masonry, r.c. | 2; 8 | AeDES | MLE | EMS-98 vulnerability classes + no. of floors; AeDES structural types; year built + no. of floors | RB/TR |
| Rosti et al. [56] | masonry, r.c. | 8 | AeDES | MLE | EMS-98 vulnerability classes; AeDES structural types + no. of floors | RB/TR |
| Rota et al. [54] | masonry, r.c. | 2; 3; 4; 5; 6 | AeDES | Levenberg-Marquardt method | AeDES structural types + no. of floors | RB/TR |
| Scala et al. [61] | masonry | 8 | AeDES | MLE | AeDES masonry quality and floor stiffness + year built + no. of floors | – |
| Zuccaro et al. [62] | masonry | 2; 4; 5; 6; 7; 8; 9 | AeDES | LSM | EMS-98 vulnerability classes | TR |
| Zucconi and Sorrentino [63] | masonry | 8 | AeDES | MLE | year built + state of maintenance + no. of floors | – |

(*) 1: Friuli 1976; 2: Irpinia 1980; 3: Abruzzo 1984; 4: Umbria-Marche 1997; 5: Pollino 1998; 6: Molise-Puglia 2002; 7: Emilia-Romagna 2003; 8: L'Aquila 2009; 9: Emilia-Romagna 2012; 10: Lunigiana 2012; 11: Central Italy 2016.
(**) Expert elicitation.

Recently, there have been efforts to systematize the many fragility models available: Yepes-Estrada et al. [44] and Rossetto et al. [19] created worldwide databases, while in Italy the IRMA platform gathers the results at national level [45,46].

Empirical fragility functions are generally regarded as more realistic because they consider all the relevant seismological factors, i.e., site amplification, soil-structure interaction, and structural and non-structural building features [19,47]. In addition, they are less affected by the conservative assumptions often implicit in mechanical models [11,37], although their validity may be limited, by region-specific structural types [48] or biases depending on their observational nature. In such context, both low and destructive earthquakes may yield few to null data, impairing the definition of the scenario.

Macroseismic scales, such as the EMS-98 [14,15] or the MCS (Mercalli – Cancani – Sieberg) [49], serve as a reference for empirical appraisal of post-earthquake damage by groups of experts, such as the QUEST or EEFIT teams[1]. These scales organize the DM in five damage grades, from D0 (negligible damage) to D5 (collapse) and the IM in discrete degrees of macroseismic intensity (I-XII). They also provide a broad classification of vulnerability: in the EMS-98, six decreasing classes are defined, from A (high vulnerability) to F (low vulnerability). Each class corresponds to a set of structural types, accounting for the variability of the strength they may express as a function of the specific building features and resisting system.

In Italy, the rapid visual assessment of damage is standardized as the AeDES form (Italian acronym for Safety and Damage Assessment in the Post-earthquake phase) to qualify the level of a building usability in the aftermath of an earthquake [50]. Nine events between 1976 and 2021[2] have been covered with this system and made available to researchers [51]. The AeDES form evaluates damage according to its severity and extension within a building; conversely, vulnerability is not directly qualified within the form, but it can be inferred *a posteriori* from the structural types defined through the masonry quality (texture and arrangement of the units), the stiffness of horizontal diaphragms (flexible, semi-rigid and rigid, see Ref. [50]) and the presence of connections (tie rods and ring beams). Damage screening is generally carried out on site; however, remote sensing applications utilizing satellite or drone images have also been proposed [47,52,53]. The main challenges highlighted by the works which use the AeDES forms to derive empirical

[1] The QUEST acronym stands for QUuick Earthquake Survey Team: it consists of a team of experts for post-earthquake macroseismic survey, aimed at supporting the Civil Protection and the Scientific Community; EEFIT stands for the Earthquake Engineering Field Investigation Team and it is a post-earthquake reconnaissance mission of English researchers after the quake of Aug. 24, 2016 in Central Italy on 42 r.c. buildings.

[2] The database includes the following seismic events: Friuli 1976, Irpinia 1980, Abruzzo 1984, Umbria-Marche 1997, Pollino 1998, Molise-Puglia 2002, Emilia-Romagna 2003, L'Aquila 2009, and Emilia-Romagna 2012.

fragility functions (Table 1; [19,24,54]) concern:

a. The damage measure:
   1. Conversion of the AeDES damage assessment, based on the extent and the structural components involved, into the EMS-98 damage grades.
   2. Neglect of undamaged or slightly damaged buildings: since the survey is conducted by request of building owners, undamaged or slightly damaged buildings are often neglected. This can lead to a bias toward more severely damaged structures.
   3. Incomplete or biased sampling: surveys may either be incomplete (e.g., external inspections only), due to safety or time constraints, or biased by less experienced surveyors who may over/underestimate the extent of damage.
   4. The effect of aftershocks and damage accumulation, which may apparently increase the damage grade.
b. The vulnerability assessment:
   1. Definition of building inventory: buildings can be grouped either in structural types, as a combination of vertical and horizontal structures, or in vulnerability classes inferred from the types. However, arbitrary definitions may yield to types not matching to actual buildings, thus obtaining unrealistic classifications.
   2. Intra-group variability: larger groups, like vulnerability classes, tend to be more dispersed than strict classifications, which may yield very similar behaviours and small variability [48].
   3. Local building traditions: outwardly similar buildings may express different behaviours in different regional contexts.
c. The intensity measure:
   1. Choice of the IM: macroseismic intensity, while informative, is affected by the subjectivity of the assessing teams, the proportionality to the vulnerability of buildings and its nature of discrete parameter [54], though it allows the comparison with the historical seismicity of an area [40]. Conversely, PGA is a physical and continuous parameter but it is locally measured and so it must be interpolated for the sites of interest.
   2. Missing IM levels: very high values of the IM may be missing or there may be an uneven distribution of IMs.
d. The statistical analysis (fitting procedure):
   1. Dependence of the calculation of cumulative probability and the subsequent fitting of fragility curves and the details of data preparation, such as binning and averaging.
   2. Underlying correlation among variables, that may bias the results.
   3. Estimation of missing data regarding structural and vulnerability features of undamaged buildings, that may come from census data, generally less detailed than AeDES ones [55,56].
   4. Handling under-sampling and over-sampling, i.e., different sizes in the input data categories (DMs or IMs).

The AeDES-based procedures presented in Table 1 (see the last column) define the structural types by considering ring beams, tie rods and floor stiffness, which may be the result of strengthening, as intrinsic features of buildings. Some combinations (e.g., tie rods and rigid floors) are improbable in new buildings, but they may be observed in existing ones, due to the superimposition of different strengthening campaigns after the first constructive phase. In general, the strengthening of masonry walls is neglected in both group definition and vulnerability classification [64].

In the common assumption, such structural elements (ties and rigid floors) are believed to always enhance the seismic behaviour of the buildings to which they are applied, thus vulnerability decreases as floors are stiffer and connections are present [65].

According to Masi et al. [11], strengthening can alter either the ductility or the strength of structures, depending on whether they affect the out-of-plane (OOP) or the in-plane (IP) behaviour. Thus, as a function of the combinations of interventions, fragility curves for fragile and ductile EMS-98 vulnerability classes were proposed. Follador et al. [34] obtained, through simulations in simplified mechanical models, fragility functions for strengthened buildings, which included grout injections or jacketing on walls and lightweight strengthening of horizontal structures (e.g., tie rods and r.c. overlays). The proposed fragility model was then compared to that obtained from expert elicitation [66].

Sandoli et al. [43] considered interventions aimed at improving connections, such as ring beams and tie rods, by means of a hybrid approach. They defined the type of intervention from expert judgment and then conducted mechanical analyses to determine the fragility parameters, considering both IP and OOP behaviours.

## 3. Materials and method

In masonry buildings in historical centres, transformations, also from a structural point of view, can be as relevant as the original conception in determining the seismic behaviour. In such context, strengthening must not be considered as a descriptor of the present condition, but a distinct parameter, capable of altering the response of a building. As observations often demonstrated that hybrid buildings had a poor seismic behaviour [67], in the following the term ‘interventions’ is used instead of ‘strengthening’ to encompass all the potential effects of these modifications on the structural behaviour of a building.

A purposely designed survey was carried out to observe such effects in the latest heavily damaging earthquakes in Italy (Central Italy, 2016), which affected an area where extensive strengthening campaigns of buildings have been implemented in a recent past (see §3.2). Structural types and vulnerability classes were created, explicitly including the effect of interventions on hybrid buildings and ensuring the compatibility with the EMS-98 scale (§3.3), and the fragility functions were obtained for both. The dataset comprises 2134 structural units (SU) as a part of 1963 ordinary masonry buildings within 19 historical centres in the 2016 seismic area (§3.4). According to MIT [68], a SU is a structurally independent part of a building, characterized by a the same loadbaering system and a continuous flow of vertical loads.


**Fig. 1.** R.c. ring beams added on historical masonry buildings: a) carved ring beam, at floor level; b) ring beam covering the whole wall thickness at roof level.

### *3.1. Methodological approach*

The methodology for obtaining the fragility functions for traditional and hybrid buildings from empirical data is summarized as follows:

1. The features of vertical and horizontal structures and the contribution of interventions (§3.2 and 3.3) determine the structural type (§4.1) and the vulnerability class (§4.2) of buildings.
2. Each building receives an overall damage grade on the EMS-98 scale from 0 to 5 (§4.3).
3. PGA is calculated through the interpolation of observed data, removing local site effects of the measuring station and including those of the location (§4.4); the correlation with macroseismic intensity is studied to assess the quality of the results.
4. PGA bins are obtained considering equal percentiles of the overall empirical cumulative distribution (§5). The empirical correlation between damage and PGA is systematized through DPMs, from which the cumulative probability is calculated. DPMs are obtained per PGA bin and both per structural type and vulnerability class, supposing that all the buildings in a location experienced the same PGA (§5.1).
5. The mean cumulative values for each PGA bin per both structural type and vulnerability class (§5.2), as well as the lower and upper bounds of the distributions, are calculated. The standard deviation $\beta$ and median PGA value $\theta$ of the fitting curves (upper, mean, lower) are determined through a non-linear least squares optimization.

The fitted curves of the vulnerability classes are then compared with other empirical fragility models available in literature (§6). The advantages of this procedure are:

1. Usage of a dedicated database created through a detailed engineering survey carried out by the same reconnaissance team, which ensures greater uniformity in data collection than AeDES-based workflows.
2. Focus on damage rather than structural safety. This avoids the damage conversion between different systems (i.e., AeDES to EMS-98) and allows to catch all the damage grades, which include negligibly or slightly damaged buildings.
3. Usage of both structural types, which show the empirical performance of similar buildings, and vulnerability classes, which allow for robust groups definition [19] and the comparison with the EMS-98.
4. Inclusion of the empirical effectiveness of interventions on historical masonry buildings when vulnerability classes and structural types are defined.

However, the following potential limitations apply to the results:

1. Damage accumulation, as surveys took place at the end of the seismic sequence.
2. The lack of a comprehensive manual for the on-site assessment. The team referred to generally available field survey techniques like AeDES, FEMA and existing reports of engineering reconnaissance of seismic damage [50,69].
3. A small number of centres and an incomplete sampling of PGA, if compared to the studies based on AeDES data (see Table 1).
4. Altered computation of the overall number of buildings where demolition of collapsed buildings and debris removal had already taken place.

### *3.2. Empirical performance of strengthened buildings*

After the 1976 Friuli earthquake and the subsequent seismic events, specific regulations were enforced in Italy for repairing and strengthening buildings already damaged or located in seismic zones [64,70,71]. To focus on Central Italy, strengthening campaigns were carried out after the earthquakes in 1972 (Ancona), 1979 (Valnerina), 1984 (Abruzzo), and 1997 (Umbria-Marche).

The goal was to achieve the box-like behaviour through rigid floors and a good connection among the floor and the walls, which primarily relied on r.c. elements, such as floor slabs and ring beams [72]. In replacing timber floors with r.c. ones, ring beams were obtained by carving the existing walls along the supports and pouring concrete within the cut, where steel rebars could have been placed. In other cases, the replaced floors were connected to the existing masonry walls through localized dovetail chases, then filled with concrete. In roofs, as they were built contextually to the replacement of the structure, ring beams covered the whole thickness of the walls (see Saretta et al. [67] and Sbrogiò et al. [71]) (Fig. 1). The strengthening of masonry walls through grouting or jacketing was


**Fig. 2.** Seismic behaviour induced by interventions on traditional masonry buildings observed in 2016 seismic area: a) IP sliding at interface between masonry and floor; b) masonry crumbling below r.c. ring beam; c) OOP mechanisms and crumbling in a building with rigid diaphragms.

**Table 2**
Empirical performance levels of masonry buildings according to the type of interventions on vertical and horizontal components and the structural detailing compared to the same building without interventions. The combinations sum up the outcomes presented in Sbrogiò et al. [71].

| Interventions on walls | Interventions on floors | Strengthening of timber floors | Replacement w/ rigid or semirigid diaphragms |
|---|---|---|---|
| **Grout injections** | Good detailing | upgrading | upgrading |
| | Poor detailing | worsening | worsening |
| **R.c. jacketing** | Good detailing | upgrading | upgrading |
| | Poor detailing | downgrading | downgrading |
| **Joint repointing** | Good detailing | improvement | improvement |
| | Poor detailing | worsening | worsening |
| **None** | - | worsening | downgrading |

not mandatory and it could be applied locally to intermediate floors or individual piers or spandrels. In common practice, the reinforcing mesh of the jackets was not connected to the ring beams, despite technical recommendations [72], and anchoring length was either neglected or insufficient. The differences in weight and stiffness between either masonry and r.c. elements or masonry with and without grouting, as well as the interruptions created in walls, cause local concentrations of inertial forces that the poor anchoring or the friction developed at the interfaces during the quakes cannot withstand. Therefore, MIT [68] underlines the importance of the compatibility in terms of weight and stiffness of the reinforcements for ensuring the box-like behaviour. The 2016 Central Italy earthquake confirmed that the interfaces between masonry and r.c. elements and the details of the reinforcement were as critical for the good seismic behaviour of hybrid buildings as masonry quality [67,73,74]. The observed outcomes ranged from very good (characterized by slight cracks due to IP and sliding mechanisms) to very poor performances (which involved masonry crumbling, OOP collapses, and 'soft story' mechanisms) (Fig. 2).

Therefore, by comparing the observed behaviour of hybrid buildings to traditional ones, the empirical effects of interventions [67, 71] was categorized as follows (compare also Table 2 and see examples in Fig. 3).

1. *Improvement*: it is achieved through light interventions on walls with good detailing (e.g., joint repointing or thick cement plaster), combined with the strengthening or replacement of floors and roofs, with proper connections to the bearing walls (steel or r.c. ring beams properly connected to walls through steel dowels).
2. *Upgrading*: it involves well-designed and detailed holistic interventions on walls, including grout injections and r.c. jacketing; floors are either replaced or reinforced, together with the insertion of roof and floor ring beams, and are properly connected to the reinforced walls.
3. *Worsening*: it includes poorly detailed light interventions on walls coupled with either the strengthening or replacement of diaphragms and r.c. ring beams, carved at floor level or covering the whole thickness of a wall at roof level, where they either simply lay on scarce quality masonry walls or are anchored through insufficient dowels.
4. *Downgrading*: it involves poorly detailed or no intervention on walls (generally of very poor quality) with the replacement of diaphragms and addition of r.c. ring beams (which are added with the same conditions of the previous category).

Table 2 highlights the role that the quality of detailing on masonry walls played in defining the empirical effect of interventions in hybrid buildings. The replacement or substitution of diaphragms with rigid floors was effective (*upgrading* or *improving*) when good


**Fig. 3.** Empirical effects of interventions on buildings: a) improvement ensured by joint repointing, strengthening of floors and tie rods; b) upgrading through masonry jacketing, tie rods and strengthening of floors; c) worsening owing to superficial repointing and replacement of floors with r.c. structures; d) downgrading caused by absence of interventions on walls and replacement of floors with r.c. slabs.

detailing of the masonry reinforcement had been ensured; vice versa, such interventions could be detrimental (*worsening* or *downgrading*).

Therefore, hybrid buildings were considered as a distinct category from the corresponding traditional type, and their vulnerability classification was not straightforward as, differently from what is currently assumed (see, e.g., the EMS-98 specifications for vulnerability classification in Refs. [14,15]), interventions not always had an improving effect on the seismic performance. Indeed, downgrading and worsening interventions acted as a vulnerability factor since they were not conceived as a holistic strengthening on the whole structure (i.e., walls, diaphragms and connections), and thus summed to more obvious ones, e.g., poor masonry quality, lack of maintenance, and transformation processes of buildings [75,76].

In this work, ring beams are implicitly considered within the reinforcement or substitution of diaphragms, whereas tie rods are excluded from the analysis due to the limited number of observations compared to those of other interventions. Moreover, tie rods did not significantly influence the seismic behaviour of buildings, often owing to poor masonry quality at the anchors or their improper layout , such as when they were installed in only one of the two main directions of a building or only at the roof level [71].

### *3.3. Building taxonomy and vulnerability classification*

The constructive features of traditional and hybrid buildings in Central Italy and the empirical performance levels connected to interventions already described led to the proposal of a specific taxonomy [71]. As a function of masonry type, three main categories are possible (Fig. 4):

- Stonework (M1), or “random rubble”, which encompasses walls constructed with randomly and sub-horizontally arranged sandstone and limestone units.
- Solid clay bricks (M2).
- Hollow clay blocks (M3).

According to their presence and effectiveness, interventions are distinguished in:

- No interventions or interventions that resulted in downgraded or worsened seismic performance (null).
- Improvement interventions (R).
- Upgrading interventions (C).

Finally, the structural types of horizontal diaphragms are classified depending on their in-plane stiffness (Fig. 5):

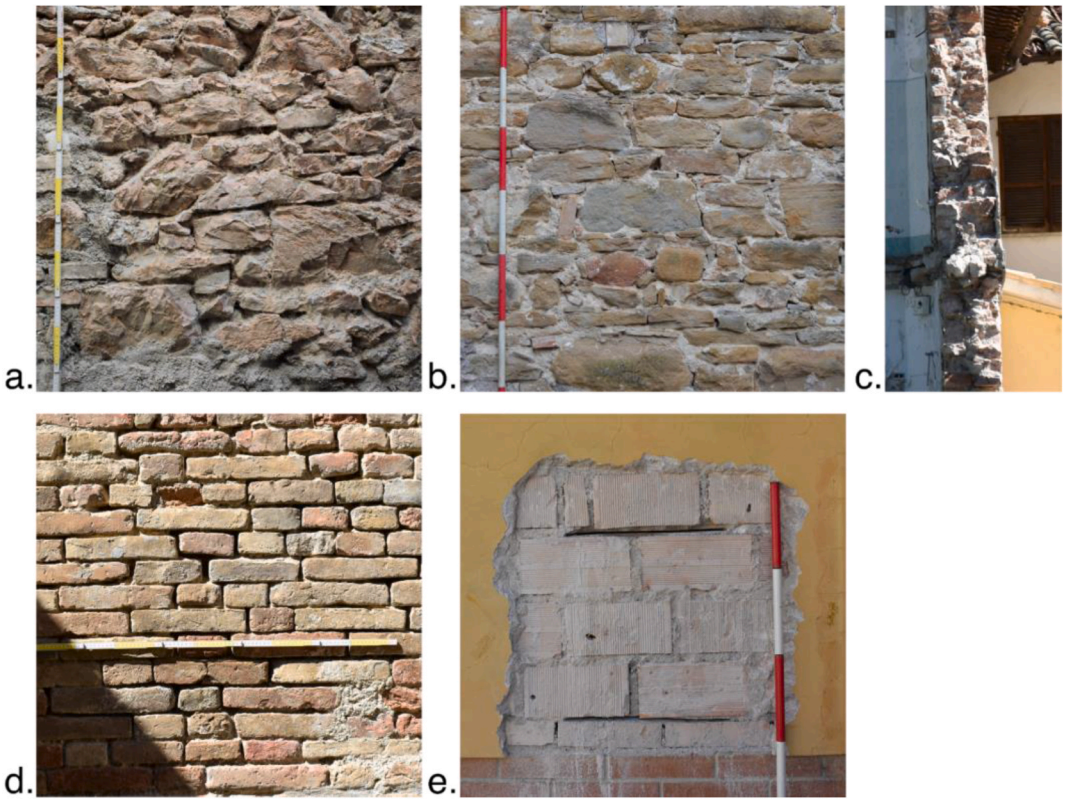


**Fig. 4.** Examples of masonry types: a) and b) random rubble masonry; c) typical stonework cross-section; d) solid clay bricks; e) hollow clay blocks.


**Fig. 5.** Examples of diaphragms: a) flexible (timber joists); b) semirigid (steel joists and clay tiles); c) semirigid ceiling (r.c. joists and clay tiles) and rigid roof (cast-in-place r.c. ribbed slab).

- Flexible diaphragms (indicated by '-F'), e.g., timber joists.
- Semirigid diaphragms (indicated by '-S'), e.g., r.c. or steel joists and clay tiles without an r.c. overlay.
- Rigid diaphragms (indicated by '-R'), e.g., cast-in-place r.c. ribbed slabs.

The taxonomic classes were obtained by appending to the masonry type (Mx) the presence/effectiveness of interventions (null, R or C) and the floor stiffness (-F, -S, -R), e.g., M1R-R is a building with improved random rubble masonry and rigid floors. The final taxonomy is shown in Table 3, where the preliminary vulnerability level, given through the shades of grey (darker is more vulnerable), is based on the empirical behaviour of types, as described in Sbrogiò et al. [71].

According to the descriptions of buildings within historical centres given in Sec. 1, structural types can be defined as:

1. Traditional buildings, i.e., M1-F and M2-F (flexible timber diaphragms with stonework and brickwork, respectively, as for the masonry type) (Fig. 6a)

**Table 3**
Building taxonomy, after Sbrogiò et al. [71]. The colours in background correspond to a level of vulnerability from the highest (dark grey) to the lowest (light grey).

| Masonry type | Interventions on walls | Diaphragms | | |
|---|---|---|---|---|
| | | flexible | semirigid | rigid |
| Stonework | None | M1-F | M1-S | M1-R |
| | Downgrading-worsening | / | | |
| Stonework | Improvement | M1R-F | M1R-S | M1R-R |
| Stonework | Upgrading | M1C-F | M1C-S | M1C-R |
| Brickwork | None | M2-F | M2-S | M2-R |
| | Downgrading-worsening | / | | |
| Brickwork | Improvement-upgrading | M2R-F | M2R-S | M2R-R |
| Hollow clay blocks | None | M3-F | M3-S | M3-R |

2. Hybrid buildings with ineffective interventions: this group includes M1-S, M1-R, M2-S and M2-R types, i.e., those traditional buildings that underwent the substitution of the original timber diaphragms with semirigid or rigid floors, without or with downgrading/worsening interventions on walls (Fig. 6b)
3. Modern buildings, i.e., M1-S, M1-R, M2-S and M2-R types, which were built starting from the 20th century with modern r.c. diaphragms but still using local stone units or bricks for masonry walls (Fig. 6c)
4. Hybrid buildings with effective interventions, which include M1R, M1C and M2R types, regardless of diaphragm stiffness; in this case, the effect of strengthening or substitution of diaphragms is positive as masonry walls were reinforced as well, with improving (M1R, M2R, Fig. 6d) or upgrading actions (M1C, Fig. 6e)
5. Recent buildings, i.e., M3 types, which were built during the last fifty years using industrialised materials for both walls (hollow clay blocks) and floors (precast r.c. joists) and according to aseismic design, although obsolete (Fig. 6f).

Further investigations into the vulnerability of these building types, according to the EMS-98, involved assigning each type to its most likely vulnerability class, given a range of likely and possible cases based on empirical performance data [65,67].

A vulnerability class is composed of different structural types with similar behaviour, i.e., reaching similar damage grades at the same intensity. Vice versa, a single type belongs to two and even three vulnerability classes with a different probability ('most likely vulnerability class', 'possible range' and 'range of less probable, exceptional cases' [14]), according to the EMS-98 Vulnerability Table.

The vulnerability classes were assigned to each structural type of the new taxonomy so that the damage distributions of A to D classes (i.e., those relevant for the assessment of masonry buildings) for the SUs in the database matched those implicitly described by the EMS-98 scale (Table 4), according to a statistic procedure described in Saretta et al. [65]. When buildings of a type belonged to a vulnerability class more than 50 % of cases, that class was the most likely; at 20–30 %, that class was probable; at less than 20 %, an exceptional vulnerability class was assigned. Such procedure applied to the present dataset obtained that:

- Types without interventions or with downgrading interventions on M1 masonry were generally the most vulnerable (class A). However, certain architectural layouts or specific structural features led to a vulnerability class B.
- M2 types were generally slightly less vulnerable and were considered as class B, especially when they featured semirigid and rigid diaphragms. However, M2 types were only observed in about 3.5 % of the sample, and thus, further refinement of their vulnerability evaluation is expected.
- Improvement interventions on M1 masonry led to a vulnerability class C.
- Upgrading interventions resulted in class D, i.e., a vulnerability level close to that of recent constructions (M3-R).

### *3.4. Building inventory*

The 2134 SUs of the dataset belong to 19 municipalities placed within the 2016 Central Italy seismic field, which was affected by three major earthquakes on Aug. 24 (Mw 6.2), Oct. 26 (Mw 6.1) and Oct. 30 (Mw 6.6), 2016 [77]. These centres were selected as a function of their distance from the epicentres, the layout of the urban environment, and the impact in terms of macroseismic intensity (Table 5). They were all built starting from the Middle Ages and suffered many earthquakes over the centuries [78], up to the events in 1979 and 1997, which stimulated extensive strengthening campaigns before the latest events.

The authors, in collaboration with a team of engineers, conducted building-by-building external inspections (95 % of the sample) between April 2018 and November 2019, at the end of the seismic sequence. They documented structural features, vulnerability and damage grades (from D0 to D5) of each SU in accordance with EMS-98. Interventions were assessed both based on the visual inspections and the perusal of archival documents and recovery plans issued after previous earthquakes, where available. On-site inspections were conducted with the support of the MUSE-DV Masonry (Multilevel assessment of SEismic Damage and Vulnerability of


**Fig. 6.** Examples of building types: a) traditional (M1-F); b) hybrid with ineffective interventions (M1-S); c) modern (M1-R); hybrid with effective interventions: d) M1R-S, e) M1C-R; f) recent (M3-R).

masonry buildings) procedure [16,17]. This rapid visual assessment form is organized into four sections of increasing detail and is tailored to evaluate the effectiveness of strengthening interventions in masonry buildings. The survey concerned the historical centre of each hamlet, focusing on the oldest masonry structures. Since it was larger than other centres and an intermediate macroseismic intensity (VII-VIII) was assessed owing to a polarization of seismic behaviour, the historical centre of Camerino was subdivided according to its historical evolution, i.e., inside (CAM-I) and outside (CAM-O) the city walls.

## 4. Data analysis

### *4.1. Structural features of buildings*

The architectural and structural features of the sampled buildings were extensively analysed in Valluzzi et al. [2]. As historical centres were mostly considered, SUs were mainly of the clustered type (30 % terraced houses, 60 % parts of cluster-blocks and just 10 % detached buildings) and low-rise heights prevailed (35 % 1-2 stories, 47 % 3 stories). Detached houses appeared in the most recent parts of the historical centres and mid-rise (4-6 stories) buildings were found mainly in the largest ones, such as CAM and AMN.

In masonry walls, stone units were typically chosen depending on local availability, with limestone and sandstone equally distributed within the sample (22 % each) and found in mountainous (ALF, CMP, CST, CLO, CSN, MCC, and PVT) and hilly (CAM, FRC, MTM, PVB, TLL) areas respectively. Travertine was typical just of ACQ and CGN and solid clay bricks were widespread only in AMN (6 %); mixed stones and bricks were often observed in CAM and FRC (24 %). In SUs built after the 1960s, hollow clay blocks were used

**Table 4**
Empirically determined vulnerability ranges for the structural types of the taxonomy according to Saretta et al. [65].

| Structural type | Vulnerability Class | | | |
|---|---|---|---|---|
| | A | B | C | D |
| M1-F | | | | |
| M1-S | | | | |
| M1-R | | | | |
| M1R-F | | | | |
| M1R-S | | | | |
| M1R-R | | | | |
| M1C-S | | | | |
| M1C-R | | | | |
| M2-F | | | | |
| M2-S | | | | |
| M2-R | | | | |
| M2R-F | | | | |
| M2R-S | | | | |
| M2R-R | | | | |
| M3-R | | | | |

Most likely vulnerability class
Probable range
Range of less probable cases

**Table 5**
Historical centres included in the empirical database, distance from the epicentres of the main seismic events, macroseismic intensities ($I_{EMS-98}$) assigned per each historical centre [79], and description of the sample size in terms of buildings and SUs.

| Historical centre, municipality (district) | ID | Earthquake | | | | | | Sample size | |
|---|---|---|---|---|---|---|---|---|---|
| | | Aug. 24, 2016 | | Oct. 26, 2016 | | Oct. 30, 2016 | | Bldgs | SUs |
| | | Distance [km] | $I_{EMS-98}$ | Distance [km] | $I_{EMS-98}$ | Distance [km] | $I_{EMS-98}$ | | |
| Acquasanta Terme (AP) | ACQ | 19 | V-VI | 35 | – | 31 | VII | 111 | 129 |
| Alfi, Valfornace (MC) | ALF | 37 | – | 13 | – | 20 | VII | 34 | 37 |
| Amandola (FM) | AMN | 31 | VI | 28 | – | 29 | VII | 216 | 253 |
| Cagnano, Acquasanta Terme (AP) | CGN | 19 | V-VI | 35 | – | 31 | VII | 35 | 43 |
| Camerino (MC) | CAM | 47 | – | 23 | – | 31 | VII-VIII | 490 | 539<br>I: 372<br>O: 221 |
| Campi Alto, Norcia (PG) | CMP | 20 | – | 5 | – | 2 | VIII | 51 | 57 |
| Capodacqua, Arquata d/T (AP) | CPD | 4 | VIII-IX | 22 | – | 16 | X | 57 | 65 |
| Castello, Valfornace (MC) | CST | 37 | – | 13 | – | 21 | VII | 16 | 23 |
| Castelluccio, Norcia (PG) | CLO | 13 | VI-VII | 14 | VI-VII | 10 | IX | 90 | 94 |
| Castelsantangelo sul Nera (MC) | CSN | 21 | VI | 6 | VIII | 8 | IX | 107 | 129 |
| Force (AP) | FRC | 37 | V-VI | 41 | – | 41 | | 100 | 128 |
| Montemonaco (AP) | MTM | 22 | V | 24 | – | 23 | VI | 37 | 43 |
| Muccia (MC) | MCC | 43 | – | 18 | VI-VII | 26 | VIII | 119 | 156 |
| Pieve Torina (MC) | PVT | 39 | – | 15 | VII-VIII | 22 | VIII | 100 | 148 |
| Pievebovigliana, Valfornace (MC) | PVB | 39 | – | 16 | – | 23 | VII-VIII | 116 | 160 |
| Piedilama, Arquata d/T (AP) | PDL | 12 | VII | 24 | – | 19 | IX | 69 | 77 |
| Pretare, Arquata d/T (AP) | PRT | 11 | VII-VIII | 24 | – | 20 | IX | 74 | 77 |
| Vezzano, Arquata d/T (AP) | VZZ | 8 | VII | 24 | – | 19 | VIII | 72 | 79 |

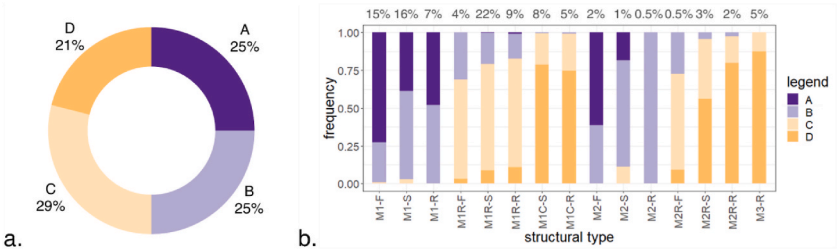


**Fig. 7.** a) Distribution of vulnerability classes within the whole sample; b) composition of classes per each structural type; distribution of structural types in the dataset at the top.

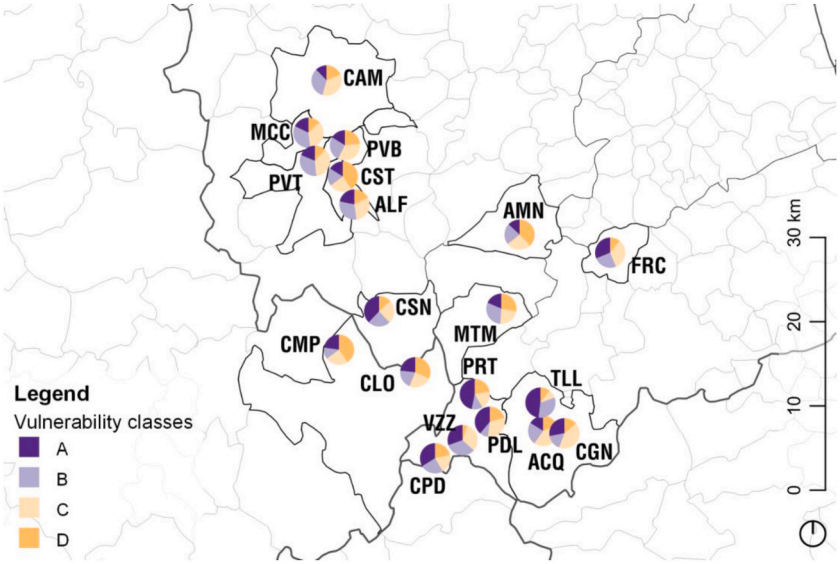


**Fig. 8.** Vulnerability classes distribution per each historical centre of the dataset.

(10 %). Rubble masonry walls were often quite thick (>40 cm) and consisted of two or three layers, usually without the use of transverse bondstones to connect them. Stone units were typically arranged in random or sub-horizontal courses, but in CAM, TLL, and MTM ashlar sporadically appeared. In general, the observed mortar quality was poor, obtained from aerial lime (26 %), also mixed with clay or mud (14 %), but 20th century block and stone walls were laid in cement mortar (29 %), and this material was also typical of joint repointing and grouting. Overall, considering the features of the mortar and the arrangement of stone units, low-quality masonry for bearing walls was widespread.

Internal horizontal structures were observed in less than half of the sample and 21 % of these were double layer timber floors. Structural masonry vaults were not recurrent (6 %), as they were part of the building tradition only in CMP, but they were found sporadically also in CSN, FRC, CAM, CPD, PRT and PDL. In the remaining cases, horizontal structures resulted from the substitution of old elements during strengthening or repair campaigns. In roofing systems, timber joists were observed in only 23 % of the sample, whereas semirigid slabs covered 46 % of cases, i.e., r.c. overlay with precast r.c. joists (19 %) or timber joists (27 %). Rigid cast-in-situ r.c. ribs were used in 24 % of the SUs. These modern roofing systems resulted mostly from the substitution of old elements, but they have been a common solution starting from the 1960s.

R.c. diaphragms were often connected to bearing walls through r.c. ring beams, chased in the perimeter walls or resting at their top. Wood or steel systems were less common. Ring beams were identified in 40 % of the buildings, of which 32 % are located at the roof level and the remainder at the floor level, although this datum may be incomplete owing to inspections from outside. Steel tie rods, which are devices traditionally chosen for connections, were present in 26 % of the SUs.

### *4.2. Building types and vulnerability classes*

Structural types were defined according to the taxonomy given in §3.2. More than a third (38 %) of the SUs fell in the M1 type, and improving actions were more common (M1R type, 35 %) than upgrading ones (M1C type, 13 %), possibly because of less economic and practical impact on buildings. M2 and M2R types were observed just in AMN, whereas the M3-R type was observed only in few cases (5 % of the sample). Semirigid diaphragms were the most common, and M1R-S was the prevalent type (22 %).

Some combinations (Table 3) of masonry type and diaphragm stiffness were not observed, such as buildings with upgraded

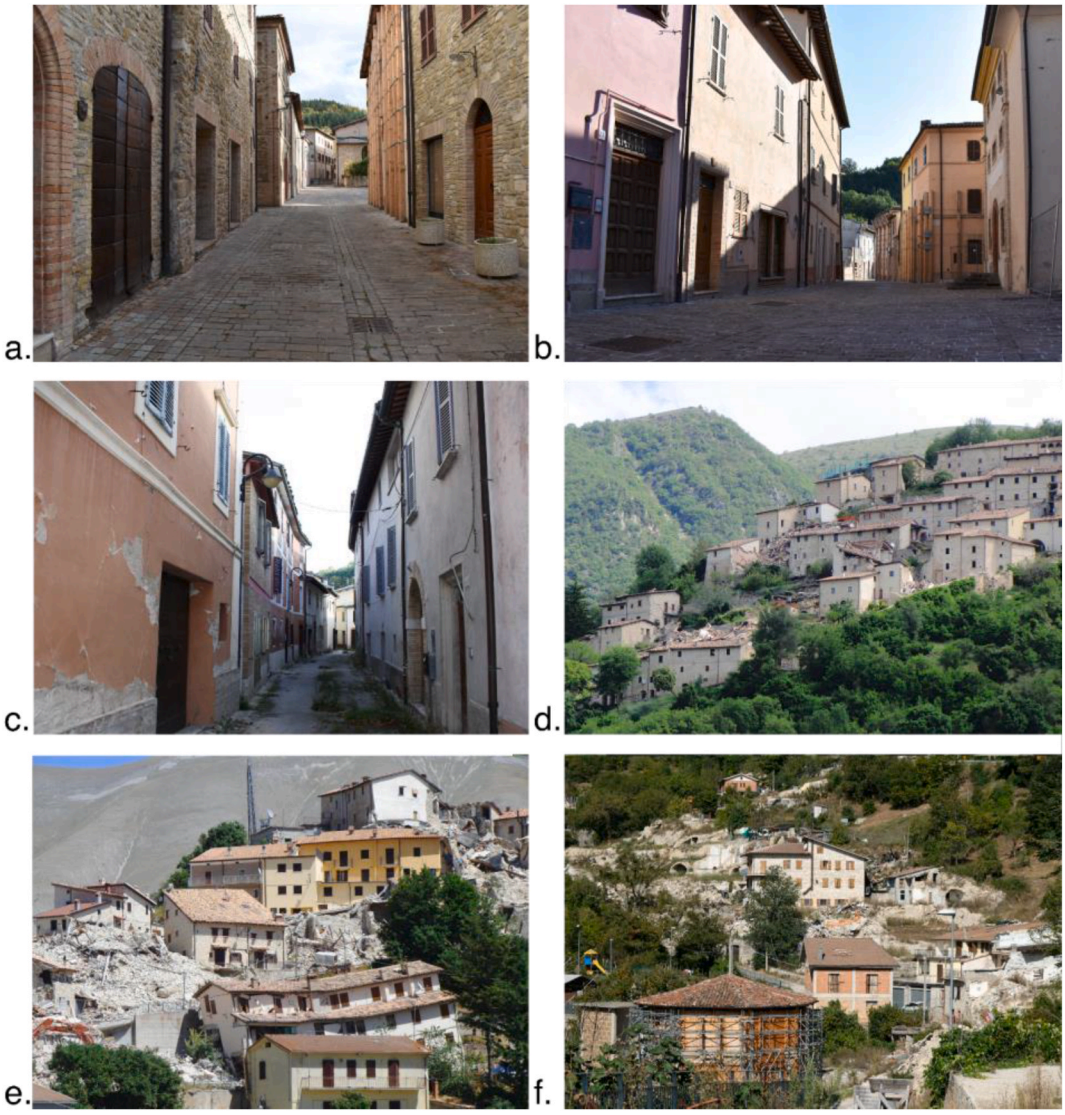


**Fig. 9.** Site survey images: view of accessible streets in historical centres far from the epicentres and with slight damage: a) PVB; b) MCC; c) PVT; panoramic view of severely damaged historical centres close to the epicentres: d) CMP; e) CLO; f) CPD.

stonework (M1C) and flexible floors (-F): typically, a comprehensive reinforcement of walls was combined with the strengthening of diaphragms. Similarly, M3-F and M3-S combinations could not be found.

Buildings were assigned to vulnerability classes according to the criteria presented in Table 4, which is an extension of the EMS-98 Vulnerability Table. Table 4 helped in choosing the class that better suited the seismic behaviour of a building: after defining its structural type, the Authors determined the most likely class and considered whether specific vulnerability conditions (e.g., quality and workmanship of masonry walls, state of conservation, plan and height regularity, position within an urban aggregate) could shift the classification to the adjacent classes. Although the choice was governed by an empirical evaluation, this approach and the experience gained on-site ensured a reasonable and robust assessment of vulnerability.

On average, the SUs in the sample were evenly distributed across the four classes (25 % in A and B, 29 % in C, 21 % in D; Fig. 7a). The types M1-F, M1-S, M1-R and M2-R, being the traditional or the worsened/downgraded buildings, were the most vulnerable and were classified only as A or B (respectively, on average, 67 and 33 % in M1-F and M2-F types, 44 and 55 % in M1-S and M1-R). B was also frequent for modern M1-S and M1-R types. In improved types (M1R, with any kind of floor, and M2R-F), the most frequent class was C (68 %, on average), followed by B (24 %); finally, upgraded types and recent buildings (M3-R) mostly fell in class D (80 %) and a few in class C (19 %) (Fig. 7b).

Fig. 8 shows the distribution of inspected buildings across classes A to D for each historical centre. In the southern centres, especially CSN, CPD, PDL, PRT, and VZZ, which were closer to the epicentres, class A was predominant (more than 30 %), but this happened also in TLL and FRC, which were further. Here, buildings were often found abandoned or in poor maintenance state and

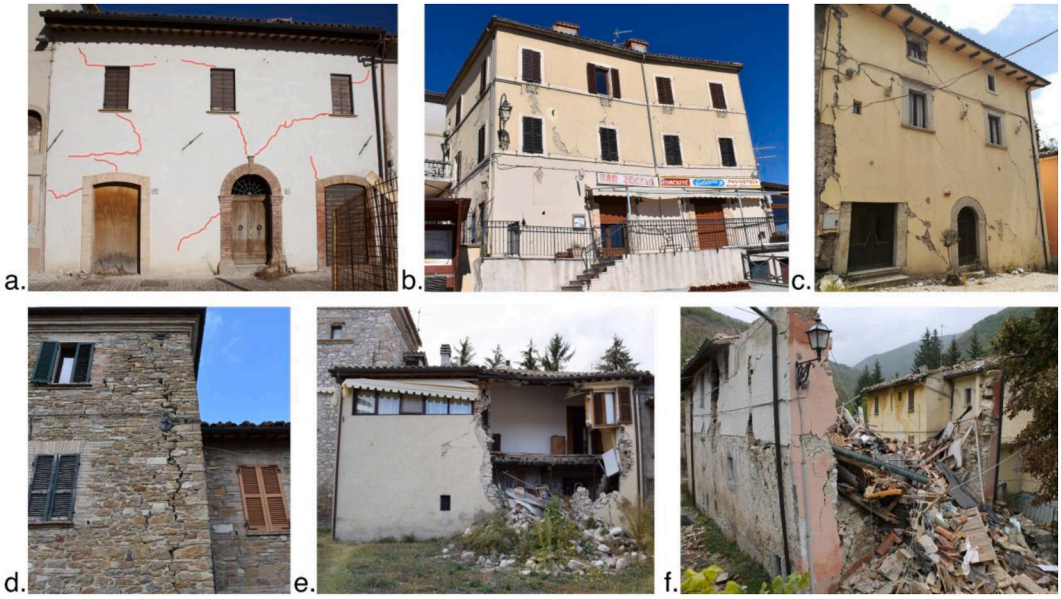


**Fig. 10.** Examples of EMS-98 damage grading to buildings within the dataset: a) D1; b) D2; c) D3 with severe shear cracks; d) D3 with triggering of a façade overturning; e) D4; f) D5.

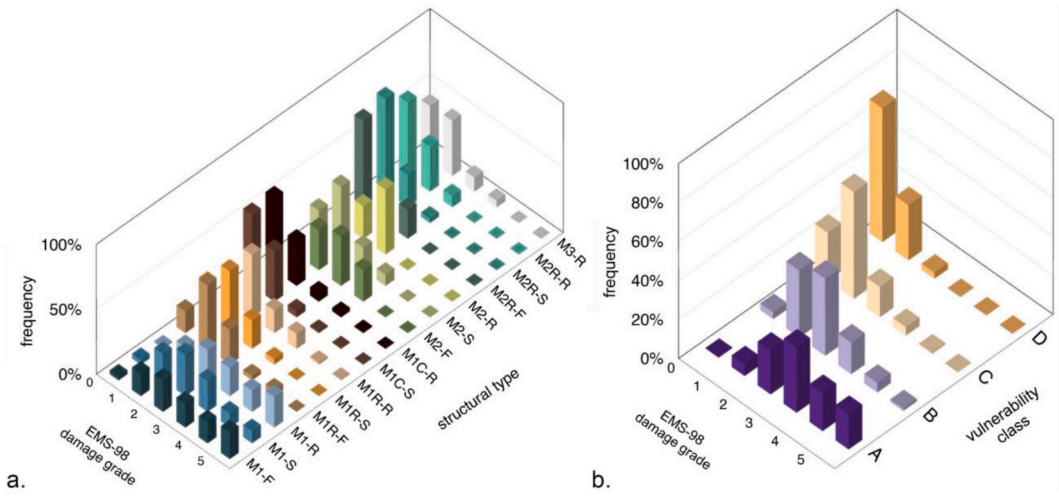


**Fig. 11.** EMS-98 damage grade distributions per: a) structural type; b) vulnerability class.

keeping their traditional conditions. High rates of class D, which resulted from interventions, were found especially in CMP (40 %) and CLO (33 %), and a significant fraction was also observed in ALF (41 %) and AMN (38 %), although in the latter case the reason was the different masonry type (M2 and M2-R). In the northern part of the analysed area, classes B and C prevailed, as joint repointing interventions were widespread.

### *4.3. Damage assessment*

Damage grades were assessed for each SU of the 19 historical centres by filling in the MUSE-DV Masonry form in front of each building, overlooking it from the outside. In historical centres with moderate to low damage, due to the distance from the epicentres (see Fig. 9a-c), it was possible to walk around buildings and, in a few cases, go inside them. In centres were the earthquake caused heavy damages and collapses, debris often obstructed the passage (see Fig. 9d-f), and inspections focused on what was visible from the accessible streets.

Damage was graded according to the EMS-98, that is in five grades from negligible or null damage (D0) to collapse (D5). D1 corresponded to very slight and concentrated cracks, generally related to IP mechanisms (shear or sliding damage). D2 graded buildings had a similar behaviour, though cracks were either slightly more evident or widespread than D1 and a slight triggering of

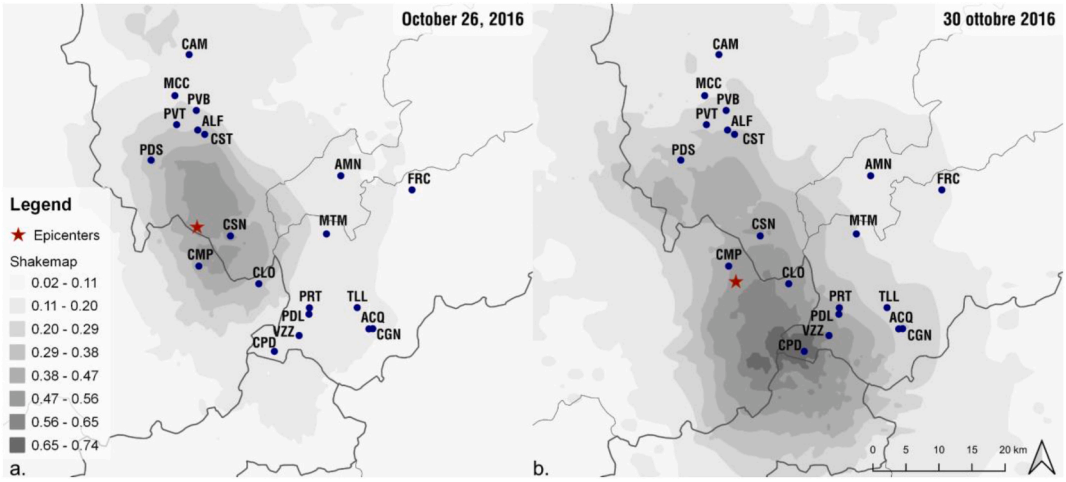


**Fig. 12.** Localization of historical centres within the shakemaps of Oct. a) 26 and b) 30, 2016 quakes (elaboration of data from Felicetta et al. [83]).

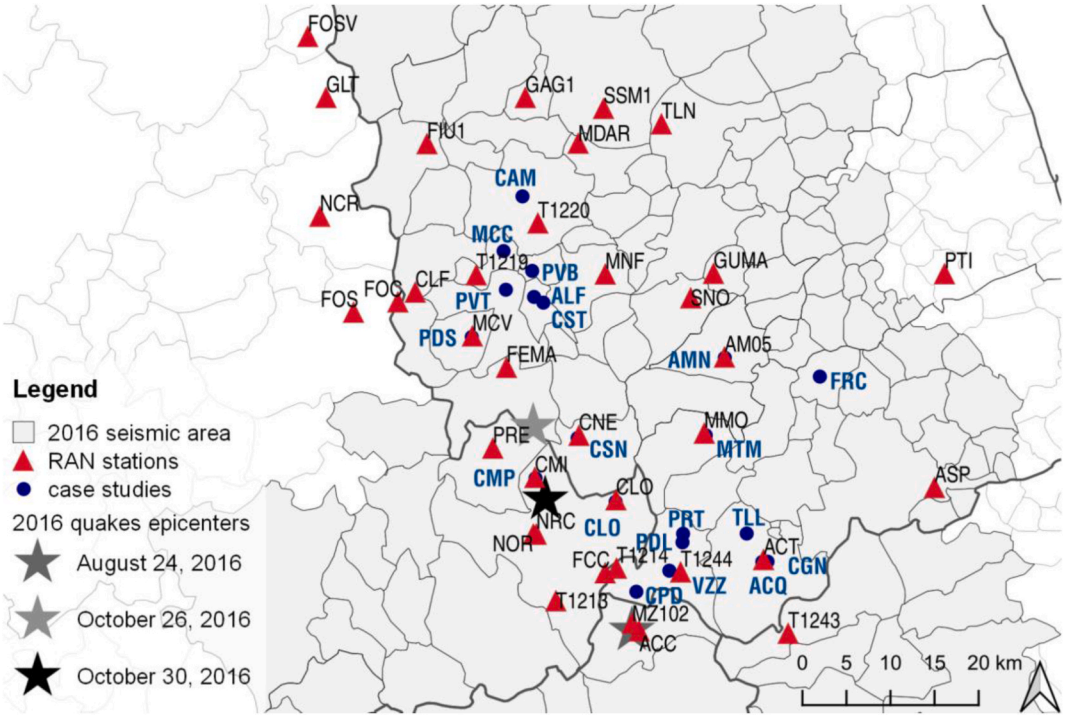


**Fig. 13.** Localization of historical centres, epicentres of the main quakes and considered stations of the RAN (the codes of the stations refer to Table A.1 in Appendix A).

OOP mechanisms was also observed. D3 was the threshold of severe damage to a structure, with the activation of OOP mechanisms on structural elements, severe shear damage in combination to masonry crumbling or overturning of non-structural parts. Buildings graded as D4 showed localized collapses by OOP mechanisms, shear damage with very severe disintegration and rigid movements of the slabs; D5 corresponded to the collapse of entire walls or collapse to rubble of whole buildings. Some examples are reported in Fig. 10.

As surveys were carried out at the end of the seismic sequence, damage grades were possibly overestimated owing to damage accumulation; conversely, in CPD and PVT some buildings were already demolished, potentially leading to an underestimation of the highest damage grades.

Fig. 11a shows the damage distribution per structural type: the most severe damages (D4 and D5) were observed in traditional stone masonry types or in hybrid buildings with downgrading interventions (M1); flexible and rigid diaphragms increased the damage. In all other types, regardless of the earthquake severity, the damage did not exceed D3. The more pervasive and comprehensive were the

**Table 6**
Soil and topography classes and values per each historical centre and $PGA_L$ obtained for the event on Oct. 30, 2016.

| ID | soil class | topography class | $S_{S,S}$ | $S_{T,L}$ | $PGA_L$ [cm/s$^2$] |
|---|---|---|---|---|---|
| MTM | A | T2 | 1.0 | 1.2 | 160.6 |
| FRC | A | T2 | 1.0 | 1.2 | 162.3 |
| CAM-O | A | T2 | 1.0 | 1.2 | 179.2 |
| CAM-I | A | T4 | 1.0 | 1.4 | 214.4 |
| ALF | A | T2 | 1.0 | 1.2 | 215.3 |
| ACQ | A | T1 | 1.0 | 1.0 | 243.2 |
| AMN | A | T2 | 1.0 | 1.2 | 251 |
| CST | A | T4 | 1.0 | 1.4 | 254.2 |
| MCC | C | T1 | 1.5 | 1.0 | 276.7 |
| PVT | C | T1 | 1.5 | 1.0 | 286.3 |
| CGN | A | T2 | 1.0 | 1.2 | 291.7 |
| TLL | A | T2 | 1.0 | 1.2 | 293.5 |
| PVB | C | T2 | 1.5 | 1.2 | 320.1 |
| CMP | A | T2 | 1.0 | 1.2 | 393.7 |
| VZZ | C | T1 | 1.5 | 1.0 | 488.1 |
| PDL | D | T1 | 1.8 | 1.0 | 544.8 |
| PRT | D | T1 | 1.8 | 1.0 | 558.4 |
| CSN | B | T2 | 1.2 | 1.2 | 582.2 |
| CLO | A | T4 | 1.0 | 1.4 | 586.9 |
| CPD | C | T1 | 1.5 | 1.0 | 721.2 |

intervention, the lesser was the damage, as expected, thus demonstrating the uniform performance of the types. Therefore, for improved stone types (M1R) and traditional solid brick types (M2), damage peaked in D1 or D2, while upgraded stone types (M1C), improved solid bricks (M2R), and hollow clay blocks (M3) suffered just very slight damage and no damage prevailed.

As regards vulnerability classes (Fig. 11b), as expected, with decreasing vulnerability from class A to D, the most frequent damage shifted of one grade towards lower values, i.e., from D3 in class A to D0 in class D. D4 and D5 were observed only for the most vulnerable buildings, with a few cases in class B (5 % and 1 % of historical centres experienced D4 and D5, respectively). Class D buildings obtained only negligible or slight damage.

### 4.4. Ground motion

The SUs were struck by three seismic events in rapid succession, with different epicentres and increasing magnitude; therefore, the observed situations combined their effects. There was a discernible increase in macroseismic intensity from the event on Aug. 24 to that on Oct. 30 and this progression correlated with an escalation in building damage grades (as discussed by Graziani et al. [80] and Rossi et al. [81]). Cumulative damage effects were particularly evident in historical centres located near the epicentres of Oct. 2016 (such as CSN, CMP, and CLO, as described by Vettore et al. [82]) but also in those that were already severely affected in August, such as CPD, PRT, and PDL, which were almost completely destroyed. The increase in local macroseismic intensity ranged between I-II degrees, i.e., from VI-VII to IX in CSN, from VIII to IX in CLO, and from VI-VII to VIII in MCC (see Table 5).

It is questionable whether the peak damage was reached either in the event with the highest local PGA or in the last one in chronological order (i.e., that on Oct. 30, 2016), which had also the largest magnitude. Looking at the shakemaps (Fig. 12), only in ALF, CST, MCC, PVT, CSN, CMP the quakes on Oct. 26 determined a higher PGA than that of Oct. 30.

This study assumed that, despite the different input acceleration between events, there was a progressive increase in vulnerability as building resistance decreased due to previous damage. Therefore, even with a decrease in demand, higher-than-expected damage occurred. As the assessment took place at the end of the sequence, this time-evolving effect on vulnerability was empirically considered through the choice of the most appropriate EMS-98 vulnerability class according to the actual behaviour (i.e., damage).

For each historical centre, the macroseismic intensity was taken from Locati et al. [79], while the shakemaps offered too broad PGA intervals. To estimate this latter parameter, the stations of the RAN (Italian acronym for National Accelerometric Network) located near the historical centres were considered (Fig. 13), as well as their soil and topography classes [84]. For the i-th station, the recorded $PGA_i$ on Oct. 30 (registered in the ITACA, acronym for ITalian ACcelerometric Archive [83]) was stripped of site effects dividing it by the subsurface ($S_{S,i}$) and topography ($S_{T,i}$) coefficients [84], to obtain the value of peak acceleration on a rigid bedrock ($a_{g,i}$) (see Table A.1 in Appendix A). The local peak acceleration on a rigid bedrock ($a_{g,L}$) was determined as the mean of the values $a_{g,i}$ measured at the four nearest stations which recorded a signal, weighted by the inverse of the distance ($d_i$). Finally, the PGA value for each location ($PGA_L$) was found multiplying $a_{g,L}$ by the subsurface and topography coefficients which characterized the location ($S_{S,L}$ and $S_{T,L}$, Table 6) (see Eq. (2), from MIT [85]).

$$PGA_L = a_{g,L} S_{S,i} S_{T,i} = \frac{\sum_{i=1}^{4} \frac{a_{g,i}}{d_i}}{\sum_{i=1}^{4} \frac{1}{d_i}} S_{S,L} S_{T,L} \quad (2)$$

It was assumed that all the SUs in a historical centre experienced the same PGA of their overall centroid and that soil conditions were constant, except for CAM, which was larger than the others. As a rule, the upper limit of the intervals defined by MIT [84] were

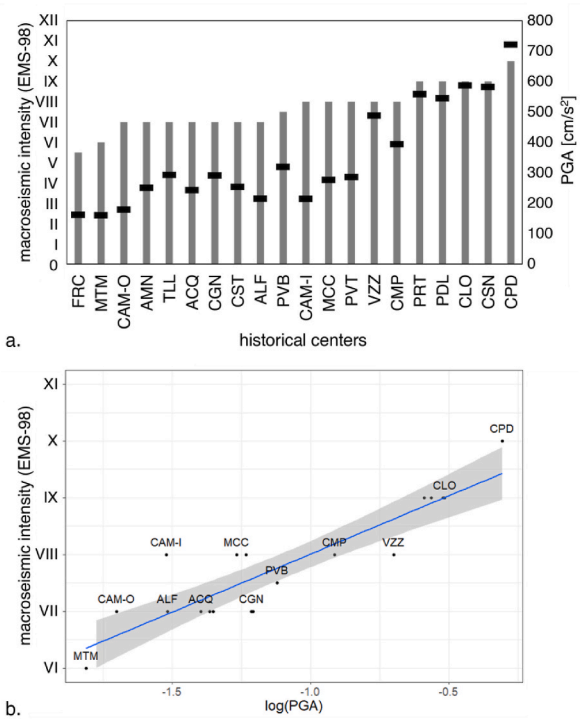


**Fig. 14.** a) Comparison and b) correlation between $I_{EMS\text{-}98}$ degrees and PGA.

**Table 7**
PGA bins for deriving fragility functions.

| PGA bin | PGA central value | No. of SU | Historical centres |
|---|---|---|---|
| [0.161,0.179) | 0.1700 | 172 | MTM, FRC |
| [0.179,0.214) | 0.1965 | 221 | CAM-O |
| [0.214,0.215) | 0.2145 | 372 | CAM-I |
| [0.215,0.251) | 0.2330 | 166 | ACQ, ALF |
| [0.251,0.277) | 0.2640 | 276 | AMN, CST |
| [0.277,0.293) | 0.2850 | 343 | CGN, MCC, PVT |
| [0.293,0.394) | 0.3435 | 237 | TLL, PVB |
| [0.394,0.582) | 0.4880 | 291 | CMP, VZZ, PDL, PRT |
| [0.582,0.721) | 0.6515 | 288 | CLO, CSN, CPD |

taken for $S_{S,L}$ and a soil class D was assumed for those centres that seismic microzonation maps marked as built on landslides deposits (PDL, PRT). Table 6 reports the results for each location ($PGA_L$).

#### 4.4.1. *Correlation between PGA and macroseismic intensity*

Fig. 14a compares the trend of macroseismic intensity ($I_{EMS\text{-}98}$) with that of PGA: the VII degree corresponds to a PGA range between 0.2 and 0.3g, the IX to the range 0.5–0.6g, while an intensity of X exceeds 0.7g. As regards the VIII degree, the PGA interval is wider, as it spans from 0.2g to 0.5g and partially covers the PGA values observed for the previous degree. In CAM-I, MCC and PVT the discrepancy between PGA and $I_{EMS\text{-}98}$ was explained by a much greater vulnerability of buildings which increased the damage; conversely, in VZZ the high PGA (0.49g) did not compare with $I_{EMS\text{-}98}$, possibly as a result of the conformation of its buildings.

As they were located on landslide deposit and despite their distance from Oct. 30 epicentre, PRT and PDL recorded a macroseismic intensity close to that of CLO and CSN, which were in the epicentral zone. In addition, the very high intensity (IX) in these centres was mainly due to damage accumulation along the events.

In order to check for the actual comparability between ground motion and damage in the historical centres, a linear correlation law log(PGA)-$I_{EMS\text{-}98}$ was estimated (Fig. 14b): a coefficient of determination equal to 0.91 and a very small p-value ($4x10^{-8}$) were obtained. The resulting equation (Eq. (3)) is similar to that proposed by Masi et al. [86], for PGA greater than 0.06g andreferring to earthquakes all over Italy.

$$I_{EMS\text{-}98} = 2.2\log(PGA) + 10 \quad (3)$$

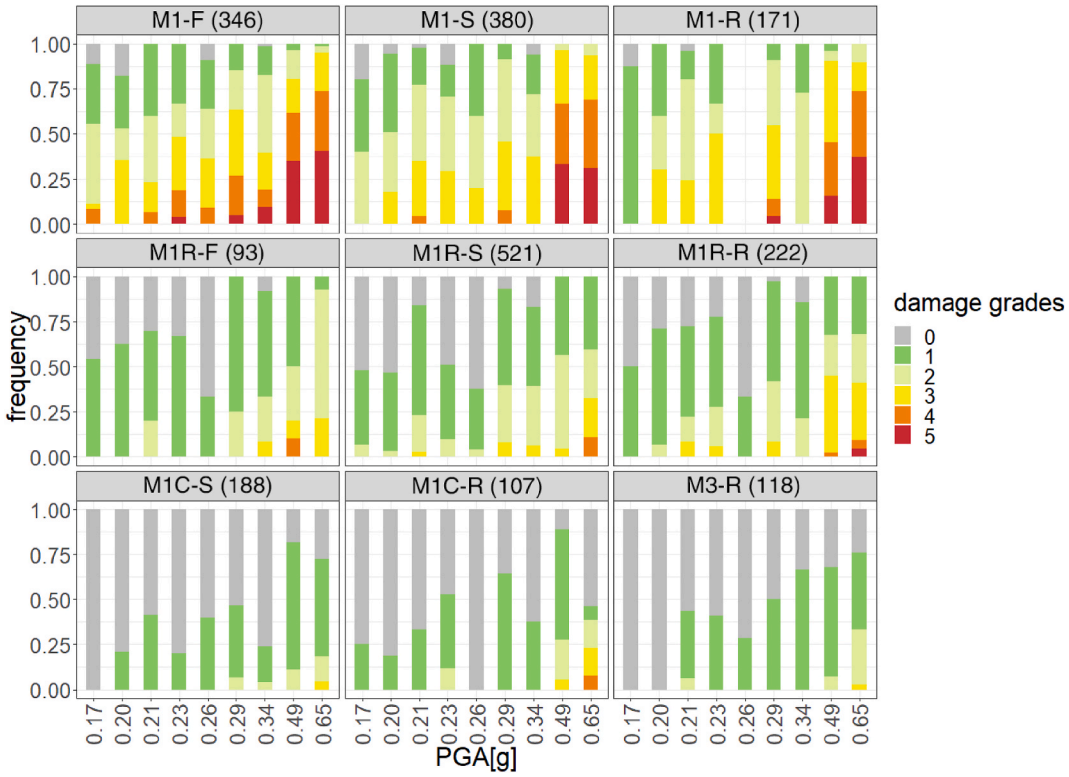


**Fig. 15.** DPM for PGA bins per each structural type (number of SU per each type is in brackets).

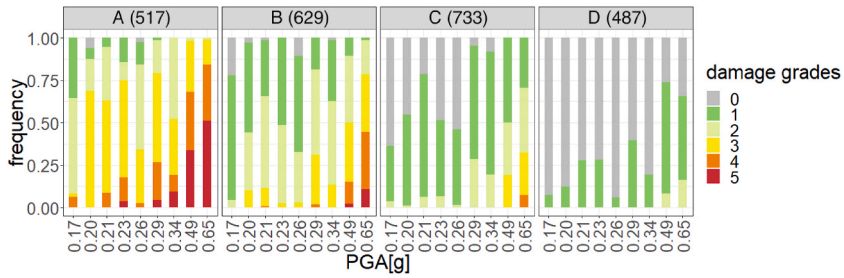


**Fig. 16.** DPM for PGA bins per each vulnerability class (number of SU per each class is in brackets).

## 5. Results

As their number varied among the historical centres, to achieve a more coherent distribution, the observed SUs were grouped into intervals of PGA, each comprising approximately 10 % of the sample. Nine PGA bins of variable width were defined, represented by their central values (Table 7): generally, they contain at least two centres, except for [0.179,0.214) and [0.214,0.215) which contain a part of CAM each. Appendix A reports the number of SUs for each vulnerability class and structural type per PGA bin (Tables A.2 and A.3).

### 5.1. Damage probability matrices

Figs. 15 and 16 show the distribution of damage levels per structural type and vulnerability class, considering the PGA bins of Table 7.

With reference to types, as the quality of interventions improved (from none or worsening, through improvement, and then upgrading, see Table 2), the damage decreased: D5 was recorded only for M1 types at PGA larger than 0.285g and in the case of M1R-R only at the highest value (0.625g); D4 appeared in every interval for M1-F, but starting from 0.285g for M1-S and M1-R types, and at the highest PGA (0.652g) in M1R and M1C-R types. M1R types were characterized by damage grades from D0 to D3, like M1C and M3-R types, although in the latter cases D0 prevailed.

As regards vulnerability classes, damage also decreased as the classes improved, both in terms of overall grade (class A reached D5

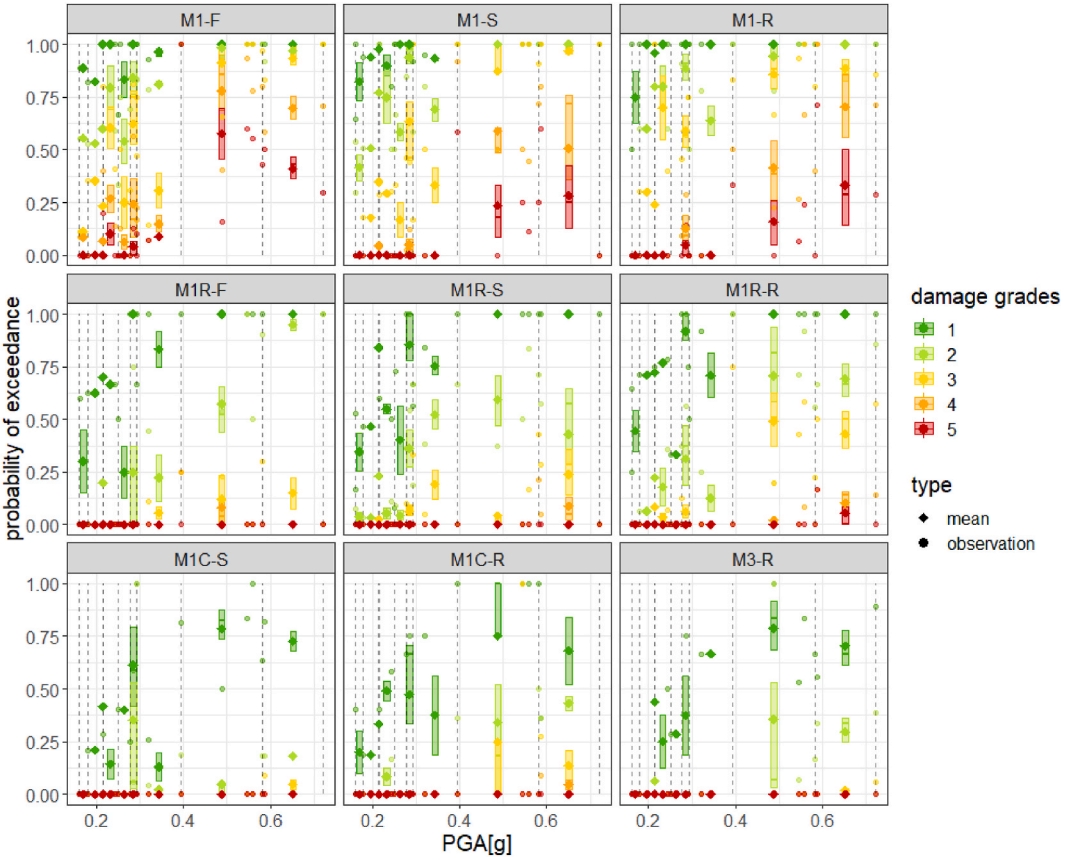


**Fig. 17.** Cumulative probability of damage exceedance per structural types and historical centre (dots); the boxplots and mean values (diamonds) refer to the PGA bins shown in Table 7. The dashed lines show the boundaries of the bins.

differently from class D) and of mean PGA at which it occurred (the D1 of class A is reached before the D1 of class B). The highest damage grades were recorded for SUs in classes A and B, especially at PGA larger than 0.233g and 0.488g, respectively. D4 in class B was observed only in four PGA bins, in one in class C, while no damage above D3 is recorded for class D.

The probability of reaching or exceeding a certain damage grade from D1 to D5, based on the PGA value, was obtained by cumulating the empirical frequency of damage from the highest to the lowest grade. The cumulative frequency of buildings that reached or exceeded each damage grade per observed historical centre, which corresponds to a PGA value, is shown by dots in Fig. 17 for structural types and in Fig. 18 for vulnerability classes. Per each PGA bin (see Table 7), delimited by dashed lines in the figures, the mean cumulative probability (diamonds in Figs. 17 and 18) and the interquartile ranges were obtained (boxplots in Figs. 17 and 18) and centered on the central value of the bin. In two bins (centered around 0.1970g and 0.2145g) there is no dispersion since only one historical centre is comprised (CAM-O and CAM-I respectively), whereas larger dispersions were computed in bins which comprised several locations, especially for PGA larger than 0.4g. This approach aims at compensating the large variability in empirical fragility at PGA level as well as the uneven distribution of PGA observations, since there are more values in the lower than the upper end of the range.

If compared to classes (Fig. 18), the dispersion of the types (Fig. 17) is generally larger, as they expressed different behaviours. Referring to the mean cumulative probability, the vulnerability of the types reduces slightly as the floors grow stiffer (from -F to -R types) and significantly as the masonry strength improves (from no reinforcement to improvement, -R, and upgrading, -C). In M1 types all the damage grades are observed, and the means move right, towards high PGA, but across the masonry type high damage grades disappears as masonry strength increases. Dispersions in probability of vulnerability classes are tighter than those of types, owing to lager groups, and a clear reduction in vulnerability is readable passing from class A to class D.

### 5.2. *Fragility functions*

In order to derive the fragility functions, a lognormal cumulative distribution (Eq. (1)) was fitted on the mean cumulative probability for each PGA bin: $\beta$ and $\theta$ of the curves were estimated through a non-linear least squares optimization [87], assuming $\beta \leq 1$. To avoid intersections between the curves, $\beta$ values were unified by averaging them either per type or class, as suggested by Porter et al. [18]. The resulting curves are shown in Figs. 19 and 20, and Tables 8 and 9 list the characteristic values of each function; D0 is not considered as its cumulative probability is one. The uncertainty in the fragility model was accounted for by fitting also the upper (more

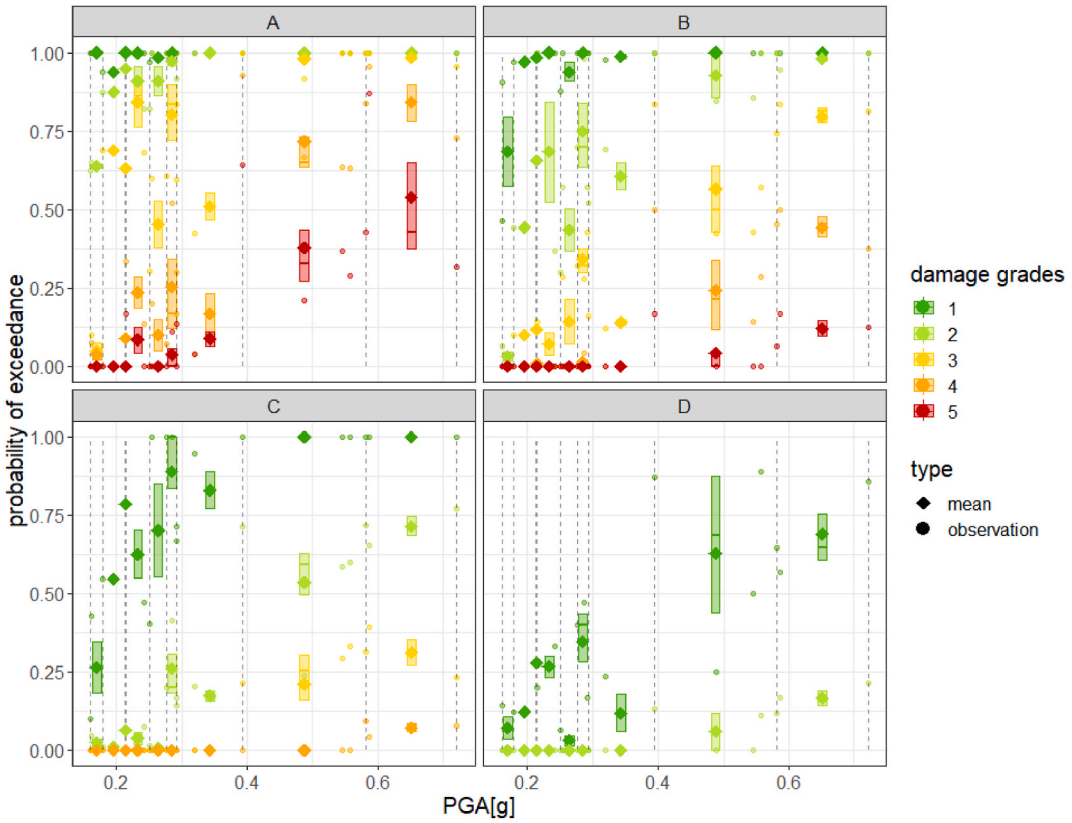


**Fig. 18.** Cumulative probability of damage exceedance per vulnerability class and historical centre (dots); the boxplots and mean values (diamonds) refer to the PGA bins shown in Table 7. The dashed lines show the boundaries of the bins.

fragile) and the lower bounds (less fragile) of the interquartile ranges of each bin (dashed lines in Figs. 19 and 20) to obtain the PGA interval at which a certain DM is met. Conversely, the variability in the vulnerability classification (see Table 4) does not affect the model, since the functions represent buildings with similar structural behaviour, empirically determined and independently from their structural type.

The reduction in dispersion of M1 curves for increasing floor stiffness without strengthened walls denounces an increasing fragility of buildings, as damage grows more rapidly with PGA. It is difficult to tell apart slight damages (D1-D2) in M1-S and M1-R types, and the estimated fragilities are very close. Severe damage conditions (D3) for random rubble (M1) types are reached for similar PGA values, independently from the floor type (0.296g, 0.321g and 0.324g for -F, -S and -R, respectively), due to the activation of local mechanism of collapse in external walls with similar severity. Near-collapse state (D4-D5) is reached by M1-F earlier than M1-S and M1-R, where stiffer floors avoid extensive collapse [67]. For improved types (M1R) the spacing of the medians as well as dispersions are much larger. At slight damage, the median PGA for D1 and D2 (about 0.2g and 0.4g) corresponds to about that of D2 and D4 in M1 types, respectively. In M1R-F and M1R-S types D4 damage is not observed and the median PGA for D3 (about 1.35g) was estimated larger than that of M1R-R (0.64g): once again, this can be explained by the incompatibility between the rigid floors and the walls, though improved, that causes extensive collapse mechanisms. The behaviour of M1C-R, if compared to that of M1C-S, can be explained in similar terms, as median D3 is estimated to be reached at the D2 of the latter (about 1.15g). Upgraded buildings show a behaviour similar to that of modern buildings (M3-R), although these latter are less dispersed (0.5g compared to 0.7g), as their construction is more homogeneous and standardized.

As regards vulnerability classes (mean fragility), a reduction in the probability of exceeding a damage grade for the same PGA level is observed for decreasing vulnerability, as expected by EMS-98. In general, a one-degree increase in median PGA for every damage grade is estimated among the classes (e.g., D1 for class B corresponds to 0.16g and D2 for class A is 0.15g). In A-rated buildings, a larger gap between the moderate (less than D3) and severe damage (D4-D5) is estimated than that among the single grades; this gap shifted to slighter damage as the vulnerability increased (between D2 and D3 in class B and between D1 and D2 in class C). This proves the increasing difficulty to reaching the threshold of severe damage in classes B-C-D, if compared to A, where extensive fragile collapses were observed. The dispersion $\beta$ for class B is the lowest, and the highest for class D. The upper and the lower bounds tend to widen as damage grades increase and, except for B-D4 and D-D2, the mean curve is centred in the reference interval. This is an effect of both the larger dispersions at higher damages and the fitting procedure, as few data are available.

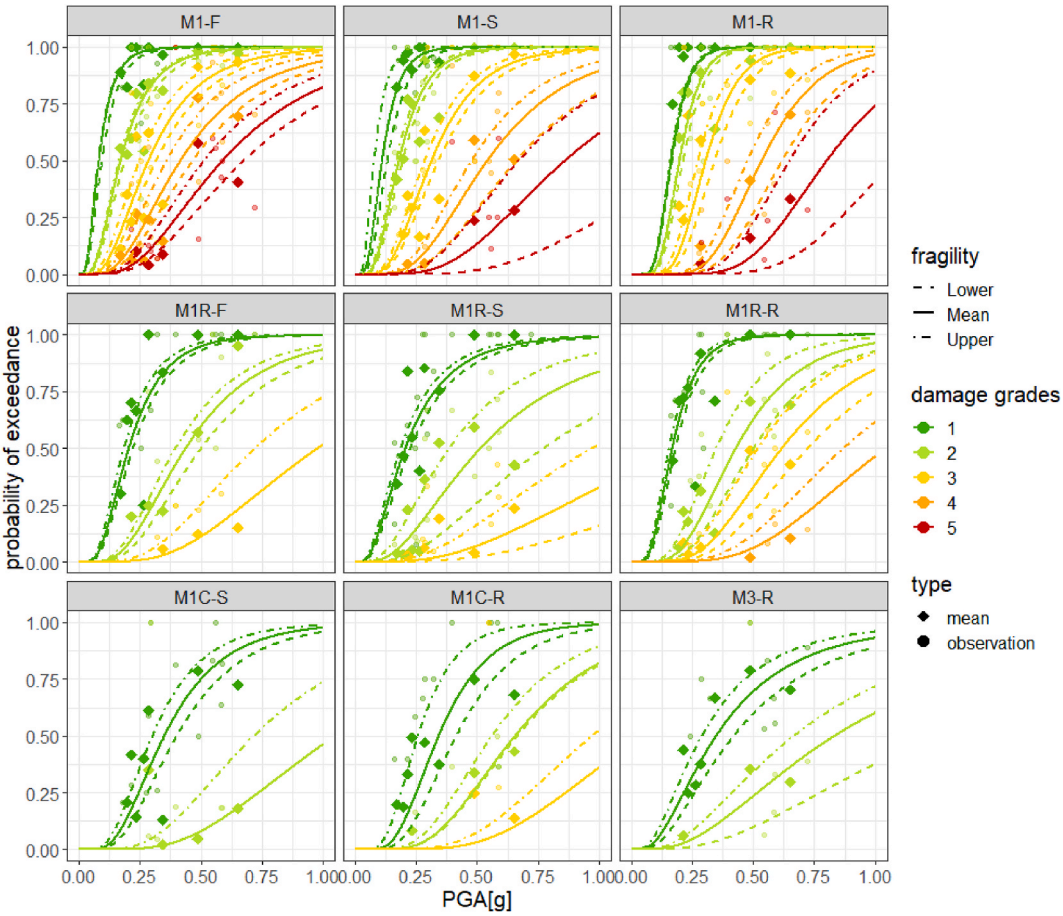


**Fig. 19.** Empirical fragility functions for structural types with and without interventions.

## 6. Discussion

The obtained fragility curves are event and region specific, as they refer to the 2016 Central Italy earthquake. However, in order to check for their broader validity, they were compared to those already proposed in literature, which consider various seismic events. As a perfect match among structural types was not possible, due to different assumptions in their definition, the comparison was carried out only for vulnerability classes. To this end, the following studies, that proposed empirical curves for A-D vulnerability classes of masonry buildings, were considered (compare Table 1):

- Masi et al. [11]: expert elicitation method, data collected through the AeDES form, nine seismic events (1976–2012) and distinction between fragile and ductile behaviour.
- Rosti et al. [56]: empirical method, data collected through the AeDES, seismic events in 1980 (Irpinia) and 2009 (L'Aquila).
- Zuccaro et al. [62]: empirical method, data collected through the AeDES form, seven seismic events (1980–2012).

As additional comparison, the EMS-98 fragility functions were also calculated, starting from the DPM proposed by Giovinazzi [41] and converting the macroseismic intensity into PGA according to Eq. (3). The fitting procedure was also that proposed by Nelder and Mead [87].

Table A.4 (see Appendix A) compares the characteristic values of the considered functions for all damage grades; in addition, a graphical comparison is made only for D2 (Fig. 21). Differently from this study, the dispersion values of Rosti et al. [56] and Masi et al. [11] are kept constants for all classes.

For class A (D2), the new model is similar to that of Masi et al. [11], while it is more fragile than that of Rosti et al. [56] and even more so than Zuccaro et al. [62] and the EMS-98. At severe damage (≥D3), the present model is intermediate among that of Masi et al. [11] (fragile) and Rosti et al. [56], and Zuccaro et al. [62] and EMS-98. At D2, the obtained dispersion is similar to Masi et al. [11] model (about 0.5–0.6).

For class B, this study is at the same time less dispersed and less fragile (0.23g ± 0.39) at D2 than Masi et al. [11] (0.19g ± 0.65) and Rosti et al. [56] (0.18g ± 0.71), whereas the model is closer to the EMS-98 (0.29g ± 0.34). Classes C and D in this study are less vulnerable than the other models. Rosti et al. [56] curve is even more fragile than Masi et al. [11], while that of EMS-98 is positioned

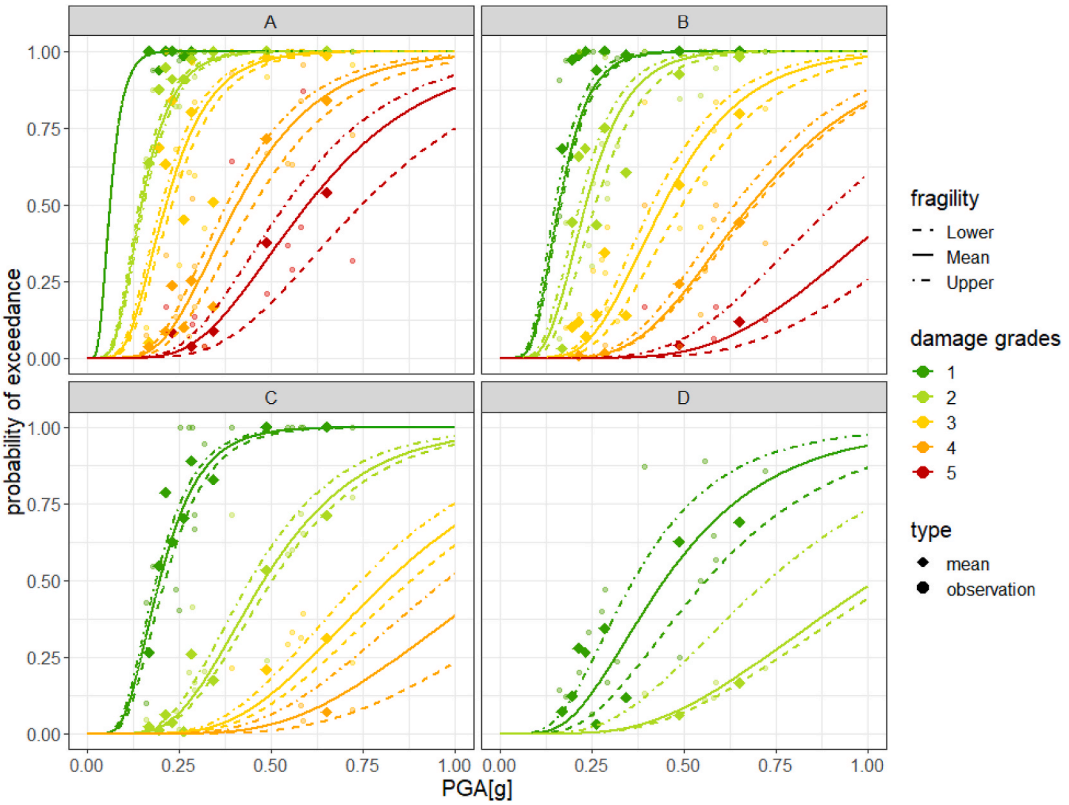


**Fig. 20.** Empirical fragility functions for EMS-98 vulnerability classes.

**Table 8**
Characteristic values of fragility functions for structural types: the values of the standard deviation ($\beta_{Di}$) and median ($\theta_{Di}$) are reported for each damage level.

| structural type | function type | $\theta_{D1}$[g] | $\beta_{D1}$[-] | $\theta_{D2}$[g] | $\beta_{D2}$[-] | $\theta_{D3}$[g] | $\beta_{D3}$[-] | $\theta_{D4}$[g] | $\beta_{D4}$[-] | $\theta_{D5}$[g] | $\beta_{D5}$[-] |
|---|---|---|---|---|---|---|---|---|---|---|---|
| M1-F | upper | 0.079 | 0.573 | 0.164 | 0.573 | 0.247 | 0.573 | 0.358 | 0.573 | 0.512 | 0.573 |
| | mean | 0.081 | 0.573 | 0.170 | 0.573 | 0.284 | 0.573 | 0.415 | 0.573 | 0.587 | 0.573 |
| | lower | 0.094 | 0.573 | 0.187 | 0.573 | 0.316 | 0.573 | 0.465 | 0.573 | 0.675 | 0.573 |
| M1-S | upper | 0.079 | 0.491 | 0.169 | 0.491 | 0.284 | 0.491 | 0.477 | 0.491 | 0.671 | 0.491 |
| | mean | 0.111 | 0.491 | 0.180 | 0.491 | 0.313 | 0.491 | 0.541 | 0.491 | 0.859 | 0.491 |
| | lower | 0.132 | 0.491 | 0.194 | 0.491 | 0.342 | 0.491 | 0.660 | 0.491 | 1.413 | 0.491 |
| M1-R | upper | 0.161 | 0.343 | 0.196 | 0.343 | 0.274 | 0.343 | 0.477 | 0.343 | 0.648 | 0.343 |
| | mean | 0.164 | 0.343 | 0.198 | 0.343 | 0.305 | 0.343 | 0.535 | 0.343 | 0.801 | 0.343 |
| | lower | 0.168 | 0.343 | 0.12 | 0.343 | 0.342 | 0.343 | 0.618 | 0.343 | 1.082 | 0.343 |
| M1R-F | upper | 0.184 | 0.550 | 0.395 | 0.550 | 0.720 | 0.550 | – | – | – | – |
| | mean | 0.204 | 0.550 | 0.436 | 0.550 | 0.977 | 0.550 | – | – | – | – |
| | lower | 0.221 | 0.550 | 0.500 | 0.550 | – | – | – | – | – | – |
| M1R-S | upper | 0.187 | 0.677 | 0.385 | 0.677 | 0.972 | 0.677 | – | – | – | – |
| | mean | 0.206 | 0.677 | 0.513 | 0.677 | 1.357 | 0.677 | – | – | – | – |
| | lower | 0.227 | 0.677 | 0.772 | 0.677 | 1.968 | 0.677 | – | – | – | – |
| M1R-R | upper | 0.156 | 0.475 | 0.349 | 0.475 | 0.519 | 0.847 | 0.869 | 0.475 | – | – |
| | mean | 0.168 | 0.475 | 0.429 | 0.475 | 0.616 | 0.475 | 1.042 | 0.475 | – | – |
| | lower | 0.182 | 0.475 | 0.501 | 0.475 | 0.722 | 0.475 | – | – | – | – |
| M1C-S | upper | 0.301 | 0.530 | 0.716 | 0.530 | – | – | – | – | – | – |
| | mean | 0.349 | 0.530 | 1.050 | 0.530 | – | – | – | – | – | – |
| | lower | 0.400 | 0.530 | – | – | – | – | – | – | – | – |
| M1C-R | upper | 0.258 | 0.462 | 0.561 | 0.462 | 0.971 | 0.462 | – | – | – | – |
| | mean | 0.342 | 0.462 | 0.655 | 0.462 | 1.178 | 0.462 | – | – | – | – |
| | lower | 0.414 | 0.462 | 0.664 | 0.462 | – | – | – | – | – | – |
| M3-R | upper | 0.290 | 0.709 | 0.667 | 0.709 | – | – | – | – | – | – |
| | mean | 0.348 | 0.709 | 0.833 | 0.709 | – | – | – | – | – | – |
| | lower | 0.420 | 0.709 | 1.250 | 0.709 | – | – | – | – | – | – |

**Table 9**
Characteristic values of fragility functions for vulnerability classes.

| class | function type | $\theta_{D1}$ [-] | $\beta_{D1}$[-] | $\theta_{D2}$[g] | $\beta_{D2}$[-] | $\theta_{D3}$[g] | $\beta_{D3}$[-] | $\theta_{D4}$[g] | $\beta_{D4}$[-] | $\theta_{D5}$[g] | $\beta_{D5}$[-] |
|---|---|---|---|---|---|---|---|---|---|---|---|
| A | upper | 0.064 | 0.438 | 0.143 | 0.438 | 0.204 | 0.438 | 0.381 | 0.438 | 0.540 | 0.438 |
| | mean | 0.064 | 0.438 | 0.149 | 0.438 | 0.216 | 0.438 | 0.408 | 0.438 | 0.599 | 0.438 |
| | lower | 0.063 | 0.438 | 0.157 | 0.438 | 0.231 | 0.438 | 0.454 | 0.438 | 0.747 | 0.438 |
| B | upper | 0.151 | 0.391 | 0.217 | 0.391 | 0.414 | 0.391 | 0.639 | 0.391 | 0.907 | 0.391 |
| | mean | 0.162 | 0.391 | 0.234 | 0.391 | 0.445 | 0.391 | 0.682 | 0.391 | 1.111 | 0.391 |
| | lower | 0.167 | 0.391 | 0.261 | 0.391 | 0.495 | 0.391 | 0.695 | 0.391 | 1.294 | 0.391 |
| C | upper | 0.189 | 0.435 | 0.444 | 0.435 | 0.745 | 0.435 | 0.976 | 0.435 | – | – |
| | mean | 0.199 | 0.435 | 0.481 | 0.435 | 0.818 | 0.435 | 1.135 | 0.435 | – | – |
| | lower | 0.213 | 0.435 | 0.504 | 0.435 | 0.881 | 0.435 | 1.374 | 0.435 | – | – |
| D | upper | 0.364 | 0.520 | 0.728 | 0.520 | – | – | – | – | – | – |
| | mean | 0.447 | 0.520 | 1.025 | 0.520 | – | – | – | – | – | – |
| | lower | 0.561 | 0.520 | 1.079 | 0.520 | – | – | – | – | – | – |

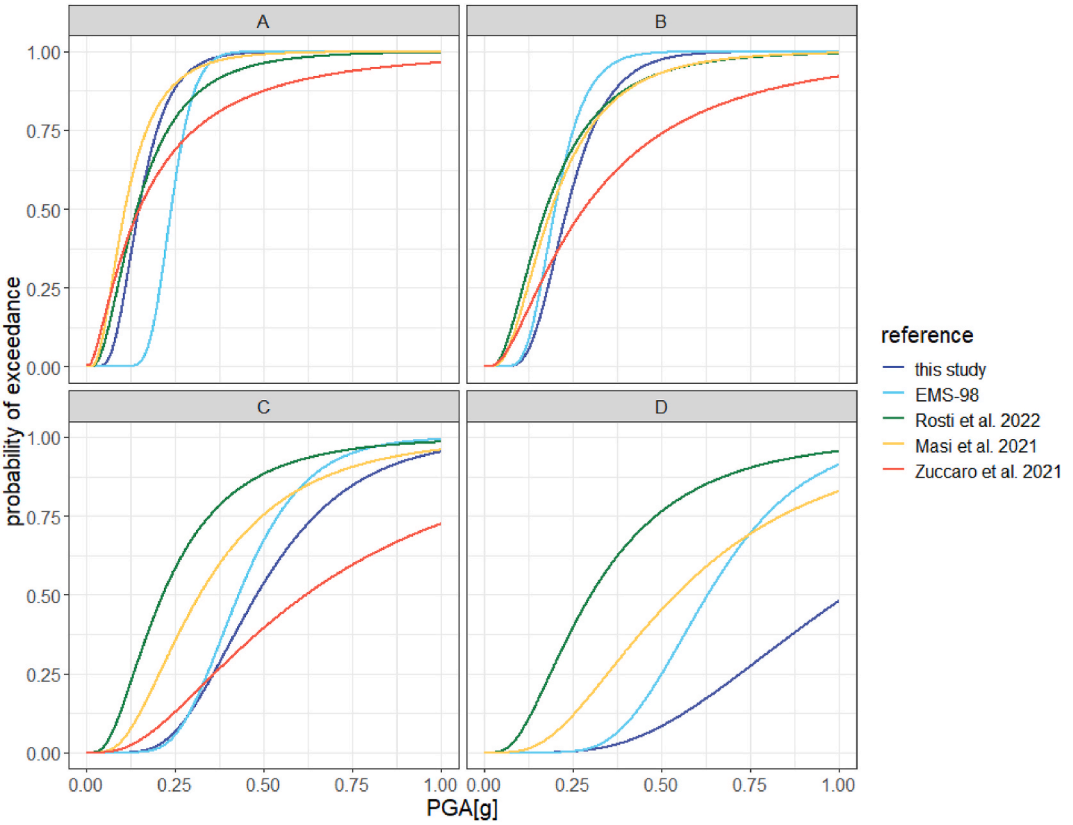


**Fig. 21.** Comparison among fragility functions for D2 proposed in this study with three literature references and the EMS-98.

halfway between the literature studies and this research; the median value of D2 in this research (0.48g) is about twice that of Rosti et al. [56] (0.22g). The same applies to D2 in class D: the median value of this study (1.03g) is three times that of Rosti et al. [56] (0.3g), twice that of Masi et al. [11] (0.54g). The dispersion values among the studies are similar in classes C and D. In this study, if compared to EMS-98 fragility, whose distance among the curves is almost constant and the dispersion is small, the median values grow more than proportionally, especially for classes C and D, where a much higher PGA is needed to reach the same probability of exceeding the previous damage level.

## 7. Conclusion

The damage patterns emerged in the 2016 Central Italy earthquake remarked that the use of r.c. interventions on traditional buildings in historical centres had two opposite effects: on one hand, holistic strengthening (e.g., the stiffening of timber floors with r.c. overlay or the integral substitution with r.c. elements, the reinforcement of walls through joint repointing or injections, and the connection of horizontal and vertical elements with ring beams) ensured a satisfactory seismic performance; on the other hand,

localized and poor quality interventions (e.g., the substitution of timber diaphragms with r.c. structures and the addition of ring beams without a proper reinforcement of bearing walls) led to severe damage and collapses, especially in buildings near the epicentres. In the latter case, buildings are defined as hybrid owing to the tampering with their original concept. Indeed, hybrid buildings had a damage threshold, in terms of PGA, higher than traditional ones, but they collapsed in a similar way. Considering that they are very diffuse in the Italian context and that they were not always able to preserve buildings from damage, interventions cannot be so effective in reducing losses to historical centres.

Consequently, the effect of r.c. interventions on the seismic performance of masonry buildings must be included within methods employed for the vulnerability and seismic risk assessment. Among those, fragility models are the basis of risk analysis and empirical ones have the advantage of considering the actual behaviour of structures to hazard. In this study, a set of empirical fragility curves was obtained for both structural types and vulnerability classes of masonry buildings in historical centres, determined over a sample of about 2134 structural units hit by the 2016 Central Italy earthquake. The dataset gathers buildings with either traditional features or interventions based on the standardized use of r.c. elements. The behaviour of hybrid buildings depended on the quality of details, compatibility with the existing structure and the extension within a building of interventions. Modern and recent buildings, i.e., those built during at the beginning of the 20th century or in the last fifty years, respectively, were also considered, albeit they were not frequent within the dataset.

Overall, nine structural types as combination of the masonry type (random rubble, brick and block masonry), floor stiffness (from flexible to rigid), and structural interventions were found, and four vulnerability classes, from A to D, were considered. Compared to others available in literature, the proposed model: i) evaluates the actual performance of buildings in historical centres, by considering both the traditional arrangement of a building and the role of strengthening interventions, also including their possible inefficacy in improving the strength of a building; ii) considers the interventions as a taxonomic criterion; iii) is based on purposely collected data, already compatible with the EMS-98 scale; iv) considers also negligibly damaged buildings and has been carried out by the same team. Possible downsides regard mainly the estimation of damage, as a sequence of earthquakes actually took place, and the buildings were inspected just from the outside. However, the comparison with other available models, which considered larger datasets, showed good compatibility, at least for the most vulnerable classes (A and B). The stronger classes (C and D) appeared as even less vulnerable than the corresponding ones in literature models, as a consequence of strengthening interventions, and class D is generally disregarded for unreinforced masonry buildings. These results confirm, on the one side, the large capacity resources of strengthened masonry buildings, but on the other, the importance of carrying out the interventions according to good design and workmanship and to explicitly include the effect of interventions in the risk analysis of existing buildings. The fragility functions here proposed contribute to improve the reliability of damage scenarios by considering the relevant structural transformations that buildings underwent in Italian historical centres.

## Funding

This project is framed within the 2022–2024 and 2024–2026 DPC-ReLUIS Project (Italian Civil Protection Department - Laboratories University Network of Seismic Engineering).

## Compliance with ethical standards

The authors declare that they have no conflict of interest.

## CRediT authorship contribution statement

**Luca Sbrogiò:** Conceptualization, Formal analysis, Investigation, Methodology, Resources, Validation, Visualization, Writing – original draft, Writing – review & editing. **Ylenia Saretta:** Conceptualization, Data curation, Formal analysis, Investigation, Methodology, Resources, Validation, Visualization, Writing – original draft, Writing – review & editing. **Maria Rosa Valluzzi:** Conceptualization, Funding acquisition, Methodology, Project administration, Resources, Supervision, Writing – review & editing.

## Declaration of competing interest

The authors declare that they have no known competing financial interests or personal relationships that could have appeared to influence the work reported in this paper.

## Data availability

Data will be made available on request.

## Acknowledgments

The authors wish to thank the Private Works Office, district of Macerata, the Municipalities of Arquata del Tronto, Acquasanta Terme, Camerino, Castelsantangelo sul Nera, Muccia, Pievebovigliana and Pieve Torina. Dr. Piatteletti and Dr. Zamengo are also acknowledged for their help in data analysis.

Photo credits: F. Molinari, Y. Saretta, L. Sbrogiò and M. Vettore.

## APPENDIX A

**Table A.1**
RAN stations and seismic action parameters recorded on Oct. 30, 2016; soil and topography classes refer to MIT [84] and were obtained from the catalogue.

| station ID | site | soil class | topography class | $PGA_i$ [cm/s$^2$] | $a_{g,i}$ [cm/s$^2$] |
|---|---|---|---|---|---|
| ACC | Accumoli | A | T1 | 425.9 | 425.9 |
| ACT | Acquasanta Terme | A | T2 | 392.7 | 242.4 |
| AM05 | Amandola | A | T1 | 270.4 | 225.3 |
| ASP | Ascoli Piceno | B | T1 | 117.6 | 98 |
| CLF | Colfiorito | B | T1 | 167.6 | 124.1 |
| CLO | Castelluccio | B | T1 | 571.4 | 414.1 |
| CMI | Campi Alto | B | T1 | – | – |
| CNE | Castelsantangelo sul Nera | B | T1 | 466.7 | 405.8 |
| FCC | Forca Canapine | A | T3 | 931.1 | 776 |
| FEMA | Monte Fema | A | T1 | – | – |
| FIU | Fiuminata | B | T1 | – | – |
| FOC | Foligno Colfiorito | C | T1 | 372.2 | 323.6 |
| FOS | Foligno Seggio | C | T1 | 116.7 | 97.2 |
| FOSV | Fossato di Vico | A | T2 | – | – |
| GAG1 | Gagliolo | B | T1 | 175 | 121.5 |
| GLT | Gualdo Tadino | B | T1 | – | – |
| GUMA | Gualdo Macerata | B | T1 | – | – |
| MCV | Monte Cavallo | B | T2 | 352.3 | 255.3 |
| MDAR | Monte Daria | B | T1 | 91.4 | 76.1 |
| MMO | Montemonaco | B | T1 | 190.4 | 132.2 |
| MNF | Monte Fiegni | A | T2 | 130.7 | 108.9 |
| MZ102 | Accumoli - Madonna delle Coste | A | T3 | 397.2 | 331 |
| NCR | Nocera Umbra | B | T1 | 190 | 135.7 |
| NOR | Norcia La Castellina | B | T1 | 305.7 | 254.8 |
| NRC | Norcia | B | T1 | 476.4 | 397 |
| PRE | Preci | A | T1 | 305 | 254.2 |
| PTI | Petritoli | A | T3 | 54.7 | 39.6 |
| SNO | Sarnano | B | T1 | 113.8 | 94.8 |
| SSM1 | San Severino Marche | B | T1 | 97.6 | 84.9 |
| T1213 | Savelli | B | T1 | 850 | 850 |
| T1214 | Forca Canapine | A | T3 | 593.2 | 411.9 |
| T1219 | Massaprofoglio | B | T1 | 268.5 | 186.4 |
| T1220 | Baregnano | B | T1 | 252.5 | 175.3 |
| T1243 | Valle Castellana | A | T4 | – | – |
| T1244 | Spelonga | A | T1 | 280.1 | 233.4 |
| TLN | Tolentino | A | T1 | 111.5 | 66.4 |

**Table A.2**
Number of SU of each EMS-98 vulnerability class for PGA bins.

| PGA central value | No. of SU | | | |
|---|---|---|---|---|
| | A | B | C | D |
| 0.1700 | 48 | 45 | 52 | 27 |
| 0.1965 | 16 | 70 | 86 | 49 |
| 0.2145 | 57 | 128 | 126 | 61 |
| 0.2330 | 28 | 37 | 62 | 39 |
| 0.2640 | 38 | 64 | 74 | 100 |
| 0.2850 | 67 | 107 | 126 | 43 |
| 0.3435 | 63 | 67 | 61 | 46 |
| 0.4880 | 106 | 46 | 78 | 61 |
| 0.6515 | 94 | 65 | 68 | 61 |
| **total** | 517 | 629 | 733 | 487 |

**Table A.3**
Number of SU of each structural type for PGA bins.

| PGA central value | No. of SU | | | | | | | | |
|---|---|---|---|---|---|---|---|---|---|
| | M1-F | M1-S | M1-R | M1R-F | M1R-S | M1R-R | M1C-S | M1C-R | M3-R |
| 0.1700 | 36 | 30 | 8 | 11 | 46 | 22 | 9 | 8 | 2 |
| 0.1965 | 17 | 51 | 10 | 8 | 60 | 31 | 24 | 16 | 3 |
| 0.2145 | 30 | 92 | 25 | 10 | 113 | 36 | 36 | 12 | 16 |
| 0.2330 | 27 | 17 | 6 | 3 | 51 | 18 | 10 | 17 | 17 |
| 0.2640 | 11 | 5 | – | 3 | 24 | 3 | 5 | 1 | 7 |

(*continued on next page*)

**Table A.3** (*continued*)

| PGA central value | No. of SU | | | | | | | | |
|---|---|---|---|---|---|---|---|---|---|
| | M1-F | M1-S | M1-R | M1R-F | M1R-S | M1R-R | M1C-S | M1C-R | M3-R |
| 0.2850 | 41 | 81 | 22 | 12 | 101 | 36 | 30 | 14 | 6 |
| 0.3435 | 63 | 32 | 11 | 12 | 66 | 14 | 25 | 8 | 6 |
| 0.4880 | 57 | 27 | 51 | 20 | 23 | 40 | 27 | 18 | 28 |
| 0.6515 | 64 | 45 | 38 | 14 | 37 | 22 | 22 | 13 | 33 |
| **total** | 346 | 380 | 171 | 93 | 521 | 222 | 188 | 107 | 118 |

**Table A.4**
Comparison of characteristic values of fragility models proposed by this study, EMS-98 and other literature works for vulnerability classes; the values of median ($\theta_{Di}$) and standard deviation ($\beta_{Di}$) are reported for each damage level. Grey background highlights values adopted to plot curves in Fig. 21.

| **EMS-98 class** | **reference** | $\theta_{D1}$ [g] | $\beta_{D1}$ [-] | $\theta_{D2}$ [g] | $\beta_{D2}$ [-] | $\theta_{D3}$ [g] | $\beta_{D3}$ [-] | $\theta_{D4}$ [g] | $\beta_{D4}$ [-] | $\theta_{D5}$ [g] | $\beta_{D5}$ [-] |
|---|---|---|---|---|---|---|---|---|---|---|---|
| A | This study | 0.064 | 0.438 | 0.149 | 0.438 | 0.216 | 0.438 | 0.408 | 0.438 | 0.599 | 0.438 |
| | EMS-98 | 0.18 | 0.24 | 0.24 | 0.21 | 0.31 | 0.29 | 0.45 | 0.4 | 0.67 | 0.38 |
| | Rosti et al. [56] | 0.087 | 0.705 | 0.143 | 0.705 | 0.176 | 0.705 | 0.241 | 0.705 | 0.447 | 0.705 |
| | Masi et al. [11] – fragile | 0.077 | 0.65 | 0.11 | 0.65 | 0.158 | 0.65 | 0.226 | 0.65 | 0.324 | 0.65 |
| | Masi et al. [11] – ductile | 0.057 | 0.65 | 0.11 | 0.65 | 0.213 | 0.65 | 0.412 | 0.65 | 0.797 | 0.65 |
| | Zuccaro et al. [62] | 0.06 | 1.05 | 0.15 | 1.05 | 0.27 | 1.05 | 0.53 | 1.05 | 1.07 | 1.05 |
| B | This study | 0.162 | 0.391 | 0.234 | 0. 391 | 0.445 | 0. 391 | 0.682 | 0. 391 | 1.111 | 0. 391 |
| | EMS-98 | 0.2 | 0.35 | 0.29 | 0.34 | 0.43 | 0.34 | 0.62 | 0.33 | 0.94 | 0.33 |
| | Rosti et al. [56] | 0.109 | 0.705 | 0.175 | 0.705 | 0.215 | 0.705 | 0.294 | 0.705 | 0.497 | 0.705 |
| | Masi et al. [11] – fragile | 0.133 | 0.65 | 0.19 | 0.65 | 0.272 | 0.65 | 0.39 | 0.65 | 0.559 | 0.65 |
| | Masi et al. [11] – ductile | 0.098 | 0.65 | 0.19 | 0.65 | 0.368 | 0.65 | 0.711 | 0.65 | 1.376 | 0.65 |
| | Zuccaro et al. [62] | 0.145 | 0.9 | 0.281 | 0.9 | 0.454 | 0.9 | 0.771 | 0.9 | 1.221 | 0.9 |
| C | This study | 0.199 | 0.435 | 0.481 | 0.435 | 0.818 | 0.435 | 1.135 | 0.435 | - | - |
| | EMS-98 | 0.29 | 0.34 | 0.43 | 0.34 | 0.62 | 0.32 | 0.87 | 0.28 | 1.26 | 0.24 |
| | Rosti et al. [56] | 0.146 | 0.705 | 0.216 | 0.705 | 0.255 | 0.705 | 0.339 | 0.705 | 0.534 | 0.705 |
| | Masi et al. [11] – fragile | 0.223 | 0.65 | 0.32 | 0.65 | 0.459 | 0.65 | 0.657 | 0.65 | 0.942 | 0.65 |
| | Masi et al. [11] – ductile | 0.165 | 0.65 | 0.32 | 0.65 | 0.619 | 0.65 | 1.198 | 0.65 | 2.318 | 0.65 |
| | Zuccaro et al. [62] | 0.234 | 0.8 | 0.619 | 0.8 | 0.794 | 0.8 | 1.297 | 0.8 | 2.27 | 0.8 |
| D | This study | 0.447 | 0.520 | 1.025 | 0.520 | - | - | - | - | - | - |
| | EMS-98 | 0.43 | 0.34 | 0.63 | 0.34 | 0.91 | 0.35 | 1.25 | 0.27 | 1.26 | 0.24 |
| | Rosti et al. [56] | 0.191 | 0.705 | 0.301 | 0.705 | 0.352 | 0.705 | 0.459 | 0.705 | 0.702 | 0.705 |
| | Masi et al. [11] – fragile | 0.377 | 0.65 | 0.54 | 0.65 | 0.774 | 0.65 | 1.109 | 0.65 | 1.59 | 0.65 |
| | Masi et al. [11] – ductile | 0.279 | 0.65 | 0.54 | 0.65 | 1.045 | 0.65 | 2.021 | 0.65 | 3.911 | 0.65 |
| | Zuccaro et al. [62] | - | - | - | - | - | - | - | - | - | - |

## References

[1] G.P. Brogiolo, A. Cagnana, Archeologia dell'architettura: metodi e interpretazioni, All'insegna del giglio, Borgo S. Lorenzo (FI), 2012.

[2] M.R. Valluzzi, L. Sbrogiò, Y. Saretta, H. Wenliuhan, Seismic response of masonry buildings in historical centres struck by the 2016 Central Italy earthquake. Impact of building features on damage evaluation, Int. J. Architect. Herit. 16 (2022) 1859–1884, https://doi.org/10.1080/15583058.2021.1916852.
[3] A. Giuffrè, A mechanical model for statics and dynamics of historical masonry buildings, in: V. Petrini, M. Save (Eds.), Prot. Archit. Herit. Earthq., Springer Vienna, Vienna, 1996, pp. 71–152, https://doi.org/10.1007/978-3-7091-2656-1_4.
[4] J. Ortega, G. Vasconcelos, H. Rodrigues, M. Correia, P.B. Lourenço, Traditional earthquake resistant techniques for vernacular architecture and local seismic cultures: a literature review, J. Cult. Herit. 27 (2017) 181–196, https://doi.org/10.1016/j.culher.2017.02.015.
[5] F. Ferrigni, Vernacular architecture: a paradigm of the local seismic culture, in: M. Correia, P.B. Lourenco, H. Varum, Seism Retrofit (Eds.), Learn Vernac Archit Seism-V Vernac. Seism. Cult. Port. Res. Proj. Funded Natl. Res. Agency FCT, CRC Press, London, 2015, pp. 3–9, https://doi.org/10.1201/b18856.
[6] R. Spence, D. D'Ayala, Damage assessment and analysis of the 1997 umbria-marche earthquakes, Struct. Eng. Int. 9 (1999) 229–233, https://doi.org/10.2749/101686699780482014.
[7] M.R. Valluzzi, On the vulnerability of historical masonry structures: analysis and mitigation, Mater. Struct. 40 (2007) 723–743, https://doi.org/10.1617/s11527-006-9188-7.
[8] M.R. Valluzzi, L. Sbrogiò, Vulnerability of architectural heritage in seismic areas: constructive aspects and effect of interventions, in: G. Amoruso, R. Salerno (Eds.), Cult. Landsc. Pract., Springer International Publishing, Cham, 2019, pp. 203–218, https://doi.org/10.1007/978-3-030-11422-0_14.
[9] V. Putrino, D. D'Ayala, Effectiveness of seismic strengthening to repeated earthquakes in historic urban contexts: norcia 2016, Disaster Prev. Manag. 29 (2019) 47–64, https://doi.org/10.1108/DPM-07-2018-0230.
[10] G. Fiorentino, A. Forte, E. Pagano, F. Sabetta, C. Baggio, D. Lavorato, C. Nuti, S. Santini, Damage patterns in the town of Amatrice after August 24th 2016 Central Italy earthquakes, Bull. Earthq. Eng. 16 (2018) 1399–1423, https://doi.org/10.1007/s10518-017-0254-z.
[11] A. Masi, S. Lagomarsino, M. Dolce, V. Manfredi, D. Ottonelli, Towards the updated Italian seismic risk assessment: exposure and vulnerability modelling, Bull. Earthq. Eng. 19 (2021) 3253–3286, https://doi.org/10.1007/s10518-021-01065-5.
[12] E. Cescatti, V. Follador, A. Prota, F. Da Porto, Development of a new seismic vulnerability model for churches based on simple typological features, Earthq. Spectra 39 (2023) 1352–1379, https://doi.org/10.1177/87552930231179741.
[13] ICOMOS, International Council on Monuments and Sites, The Valletta Principles for the Safeguarding and Management of Historic Cities, Towns and Urban Areas, Adopted by the 17th ICOMOS General Assembly on, 28 November 2011.
[14] G. Grünthal (Ed.), European Macroseismic Scale 1998: EMS-98, second ed.European Seismological Commission, Subcommission on Engineering Seismology, Working Group Macroseismic scales, Luxembourg, 1998.
[15] G. Grünthal, A. Tertulliani, R. Azzaro, G. Buffarini, Scala Macrosismica Europea 1998, EMS-98, European Seismological Commission, Subcommission on Engineering Seismology, Working Group Macroseismic scales, Luxembourg, 2019.
[16] Y. Saretta, L. Sbrogiò, F. Molinari, M. Vettore, M.R. Valluzzi, Proposta di un nuovo strumento multilivello per la valutazione del danno e della vulnerabilità a scala urbana: la procedura MUSE-DV masonry per la valutazione empirica del comportamento di edifici consolidati, Progett. Sismica 12 (2020) 5–30, https://doi.org/10.7414/PS.12.1.1.
[17] L. Sbrogiò, Y. Saretta, F. Molinari, M.R. Valluzzi, Multilevel assessment of seismic damage and vulnerability of masonry buildings (MUSE-DV) in historical centers: development of a mobile android application, Sustainability 14 (2022) 7145, https://doi.org/10.3390/su14127145.
[18] K. Porter, R. Kennedy, R. Bachman, Creating fragility functions for performance-based earthquake engineering, Earthq. Spectra 23 (2007) 471–489, https://doi.org/10.1193/1.2720892.
[19] T. Rossetto, I. Ioannou, D.N. Grant, Existing Empirical Fragility and Vulnerability Functions: Compendium and Guide for Selection, GEM Foundation, Pavia, Italy, 2015.
[20] V. Silva, H. Crowley, M. Pagani, D. Monelli, R. Pinho, Development of the OpenQuake engine, the Global Earthquake Model's open-source software for seismic risk assessment, Nat. Hazards 72 (2014) 1409–1427, https://doi.org/10.1007/s11069-013-0618-x.
[21] K. Porter, A Beginner's Guide to Fragility, Vulnerability, and Risk, University of Colorado, Boulder, 2020. https://www.sparisk.com/pubs/Porter-beginners-guide.pdf.
[22] C. Del Gaudio, G. de Martino, M. Di Ludovico, G. Manfredi, A. Prota, P. Ricci, G.M. Verderame, Empirical fragility curves from damage data on RC buildings after the 2009 L'Aquila earthquake, Bull. Earthq. Eng. 15 (2017) 1425–1450, https://doi.org/10.1007/s10518-016-0026-1.
[23] R.V. Whitman, J. Reed, S. Hong, Earthquake damage probability matrices, in: Proc. 5th World Conf. Earthq. Eng. Rome Italy June 25-29, 1973.
[24] A. Rosti, M. Rota, A. Penna, Empirical fragility curves for Italian URM buildings, Bull. Earthq. Eng. 19 (2021) 3057–3076, https://doi.org/10.1007/s10518-020-00845-9.
[25] A.G. Simões, R. Bento, S. Lagomarsino, S. Cattari, P.B. Lourenço, Fragility functions for tall URM buildings around early 20th century in Lisbon, Part 2: application to different classes of buildings, Int. J. Architect. Herit. 15 (2021) 373–389, https://doi.org/10.1080/15583058.2019.1661136.
[26] S. Taffarel, M. Caliman, M.R. Valluzzi, F. da Porto, C. Modena, Seismic vulnerability assessment of clustered historical centers: fragility curves based on local collapse mechanisms analyses, in: C. Modena, F. da Porto, M. Valluzzi, Block Mason Brick (Eds.), Proc. 16th Int. Brick Block Mason. Conf. Padova Italy 26-30 June 2016, CRC Press, 2016, pp. 2463–2470, https://doi.org/10.1201/b21889.
[27] A.H. Barbat, L.G. Pujades, N. Lantada, Seismic damage evaluation in urban areas using the capacity spectrum method: application to Barcelona, Soil Dynam. Earthq. Eng. 28 (2008) 851–865, https://doi.org/10.1016/j.soildyn.2007.10.006.
[28] N. Chieffo, F. Clementi, A. Formisano, S. Lenci, Comparative fragility methods for seismic assessment of masonry buildings located in Muccia (Italy), J. Build. Eng. 25 (2019) 100813, https://doi.org/10.1016/j.jobe.2019.100813.
[29] P. Lamego, P.B. Lourenço, M.L. Sousa, R. Marques, Seismic vulnerability and risk analysis of the old building stock at urban scale: application to a neighbourhood in Lisbon, Bull. Earthq. Eng. 15 (2017) 2901–2937, https://doi.org/10.1007/s10518-016-0072-8.
[30] M. Angiolilli, A. Brunelli, S. Cattari, Fragility curves of masonry buildings in aggregate accounting for local mechanisms and site effects, Bull. Earthq. Eng. 21 (2023) 2877–2919, https://doi.org/10.1007/s10518-023-01635-9.
[31] M. Rota, A. Penna, G. Magenes, A methodology for deriving analytical fragility curves for masonry buildings based on stochastic nonlinear analyses, Eng. Struct. 32 (2010) 1312–1323, https://doi.org/10.1016/j.engstruct.2010.01.009.
[32] V. Manfredi, A. Masi, G. Nicodemo, A. Digrisolo, Seismic fragility curves for the Italian RC residential buildings based on non-linear dynamic analyses, Bull. Earthq. Eng. 21 (2023) 2173–2214, https://doi.org/10.1007/s10518-022-01605-7.
[33] M. Donà, P. Carpanese, V. Follador, L. Sbrogiò, F. da Porto, Mechanics-based fragility curves for Italian residential URM buildings, Bull. Earthq. Eng. 19 (2021) 3099–3127, https://doi.org/10.1007/s10518-020-00928-7.
[34] V. Follador, P. Carpanese, M. Donà, F. Da Porto, Effect of retrofit interventions on seismic fragility of Italian residential masonry buildings, Int. J. Disaster Risk Reduc. 91 (2023) 103668, https://doi.org/10.1016/j.ijdrr.2023.103668.
[35] D. D'Ayala, E. Kishali, Global vulnerability estimation methods for the global earthquake model, in: 15th World Conf. Eartquake Eng. Sept. 24-28 Lisb, Port., 2012.
[36] B. Borzi, H. Crowley, R. Pinho, Simplified pushover-based earthquake loss assessment (SP-bela) method for masonry buildings, Int. J. Architect. Herit. 2 (2008) 353–376, https://doi.org/10.1080/15583050701828178.
[37] M. Colombi, B. Borzi, H. Crowley, M. Onida, F. Meroni, R. Pinho, Deriving vulnerability curves using Italian earthquake damage data, Bull. Earthq. Eng. 6 (2008) 485–504, https://doi.org/10.1007/s10518-008-9073-6.
[38] A. Blyth, B. Di Napoli, F. Parisse, Z. Namourah, E. Anglade, A.-M. Giatreli, H. Rodrigues, T.M. Ferreira, Assessment and mitigation of seismic risk at the urban scale: an application to the historic city center of Leiria, Portugal, Bull. Earthq. Eng. 18 (2020) 2607–2634, https://doi.org/10.1007/s10518-020-00795-2.
[39] K.S. Jaiswal, W.P. Aspinall, D. Perkins, D. Wald, K.A. Porter, Use of expert judgment elicitation to estimate seismic vulnerability of selected building types, in: 15th World Conf. Earthquake Eng. Sept. 24-28 Lisb, Port., 2012.
[40] S. Lagomarsino, S. Cattari, D. Ottonelli, The heuristic vulnerability model: fragility curves for masonry buildings, Bull. Earthq. Eng. 19 (2021) 3129–3163, https://doi.org/10.1007/s10518-021-01063-7.

[41] S. Giovinazzi, The Vulnerability Assessment and the Damage Scenario in Seismic Risk Analysis, University of Braunschweig (Germany), 2005, https://doi.org/10.24355/DBBS.084-200511080100-312.
[42] V. Cardinali, M. Tanganelli, R. Bento, A hybrid approach for the seismic vulnerability assessment of the modern residential masonry buildings, Int. J. Disaster Risk Reduc. 79 (2022) 103193, https://doi.org/10.1016/j.ijdrr.2022.103193.
[43] A. Sandoli, G.P. Lignola, B. Calderoni, A. Prota, Fragility curves for Italian URM buildings based on a hybrid method, Bull. Earthq. Eng. 19 (2021) 4979–5013, https://doi.org/10.1007/s10518-021-01155-4.
[44] C. Yepes-Estrada, V. Silva, D. D'Ayala, T. Rossetto, I. Ioannou, A. Meslem, H. Crowley, GEM vulnerability database, Earthq. Spectra 32 (2016) 2567–2585, https://doi.org/10.13117/GEM.DATASET.VULN.WEB-V1.0.
[45] B. Borzi, M. Onida, M. Faravelli, D. Polli, M. Pagano, D. Quaroni, A. Cantoni, E. Speranza, C. Moroni, IRMA platform for the calculation of damages and risks of Italian residential buildings, Bull. Earthq. Eng. 19 (2020), https://doi.org/10.1007/s10518-020-00924-x.
[46] F. da Porto, M. Donà, A. Rosti, M. Rota, S. Lagomarsino, S. Cattari, B. Borzi, M. Onida, D. De Gregorio, F.L. Perelli, C. Del Gaudio, P. Ricci, E. Speranza, Comparative analysis of the fragility curves for Italian residential masonry and RC buildings, Bull. Earthq. Eng. 19 (2021) 3209–3252, https://doi.org/10.1007/s10518-021-01120-1.
[47] A. Miano, F. Jalayer, G. Forte, A. Santo, Empirical fragility assessment using conditional GMPE-based ground shaking fields: application to damage data for 2016 Amatrice Earthquake, Bull. Earthq. Eng. 18 (2020) 6629–6659, https://doi.org/10.1007/s10518-020-00945-6.
[48] S. Lagomarsino, S. Cattari, Fragility functions of masonry buildings, in: K. Pitilakis, H. Crowley, A.M. Kaynia (Eds.), SYNER-G Typology Defin. Fragility Funct. Phys. Elem. Seism. Risk, Springer Netherlands, Dordrecht, 2014, pp. 111–156, https://doi.org/10.1007/978-94-007-7872-6_5.
[49] A. Sieberg, Geologie der Erdbeben, Handb, Geophys. 2 (1930) 552–555.
[50] C. Baggio, A. Bernardini, R. Colozza, L. Corazza, M. dalla Bella, G.D. Pasquale, M. Dolce, A. Goretti, A. Martinelli, G. Orsini, F. Papa, G. Zuccaro, M. Rota, A. Goretti, Field Manual for post-earthquake damage and safety assessment and short term countermeasures, in: AeDES, A.V. Pinto, F. Taucer (Eds.), Translation from Italian, JRC-DPC, 2007.
[51] M. Dolce, E. Speranza, F. Giordano, B. Borzi, C. Conte, A. di Meo, M. Faravelli, V. Pascale, D.O. WebGIS, Observed damage database of past Italian earthquakes: the Da, Boll. Geofis. Teor. Ed Appl. 60 (2019) 141–164, https://doi.org/10.4430/bgta0254.
[52] F. Piccinini, A. Gorreja, F. Di Stefano, R. Pierdicca, L.J. Sanchez Aparicio, E.S. Malinverni, Preservation of villages in Central Italy: geomatic techniques' integration and GIS strategies for the post-earthquake assessment, ISPRS Int. J. Geo-Inf. 11 (2022) 291, https://doi.org/10.3390/ijgi11050291.
[53] V. Croce, G. Caroti, A. Piemonte, Assessment of earthquake-induced damage level on buildings: analysis of two different survey methods for a case study, ISPRS - Int. Arch. Photogramm. Remote Sens. Spat. Inf. Sci. Vol. XLII-2W15 2019 27th CIPA Int. Symp. "Documenting Past Better Futur. Ávila Spain Sept (2019) 351–358, https://doi.org/10.5194/isprs-archives-XLII-2-W15-351-2019.
[54] M. Rota, A. Penna, C.L. Strobbia, Processing Italian damage data to derive typological fragility curves, Soil Dynam. Earthq. Eng. 28 (2008) 933–947, https://doi.org/10.1016/j.soildyn.2007.10.010.
[55] I. Ioannou, S. Bertelli, E. Verrucci, V. Arcidiacono, T. Rossetto, Empirical fragility assessment of residential buildings using data from the Emilia 2012 sequence of earthquakes, Bull. Earthq. Eng. 19 (2021) 1765–1795, https://doi.org/10.1007/s10518-021-01047-7.
[56] A. Rosti, M. Rota, A. Penna, An empirical seismic vulnerability model, Bull. Earthq. Eng. 20 (2022) 4147–4173, https://doi.org/10.1007/s10518-022-01374-3.
[57] F. De Luca, G.E.D. Woods, C. Galasso, D. D'Ayala, RC infilled building performance against the evidence of the 2016 EEFIT Central Italy post-earthquake reconnaissance mission: empirical fragilities and comparison with the FAST method, Bull. Earthq. Eng. 16 (2018) 2943–2969, https://doi.org/10.1007/s10518-017-0289-1.
[58] C. Del Gaudio, M. Di Ludovico, M. Polese, G. Manfredi, A. Prota, P. Ricci, G.M. Verderame, Seismic fragility for Italian RC buildings based on damage data of the last 50 years, Bull. Earthq. Eng. 18 (2020) 2023–2059, https://doi.org/10.1007/s10518-019-00762-6.
[59] G. Menichini, V. Nistri, S. Boschi, E. Del Monte, M. Orlando, A. Vignoli, Calibration of vulnerability and fragility curves from moderate intensity Italian earthquake damage data, Int. J. Disaster Risk Reduc. 67 (2022) 102676, https://doi.org/10.1016/j.ijdrr.2021.102676.
[60] A. Rosti, C. Del Gaudio, M. Di Ludovico, G. Magenes, A. Penna, M. Polese, A. Prota, P. Ricci, M. Rota, G.M. Verderame, Empirical vulnerability curves for Italian residential buildings, Boll. Geofis. Teor. Ed Appl. 61 (2020), https://doi.org/10.4430/bgta0311.
[61] S.A. Scala, C. Del Gaudio, G.M. Verderame, Towards a multi-parametric fragility model for Italian masonry buildings based on the informative level, Structures 59 (2024) 105613, https://doi.org/10.1016/j.istruc.2023.105613.
[62] G. Zuccaro, F.L. Perelli, D. De Gregorio, F. Cacace, Empirical vulnerability curves for Italian mansory buildings: evolution of vulnerability model from the DPM to curves as a function of accelertion, Bull. Earthq. Eng. 19 (2021) 3077–3097, https://doi.org/10.1007/s10518-020-00954-5.
[63] M. Zucconi, L. Sorrentino, Census-based typological damage fragility curves and seismic risk scenarios for unreinforced masonry buildings, Geosciences 12 (2022) 45, https://doi.org/10.3390/geosciences12010045.
[64] R. Sisti, M. Di Ludovico, A. Borri, A. Prota, Damage assessment and the effectiveness of prevention: the response of ordinary unreinforced masonry buildings in Norcia during the Central Italy 2016–2017 seismic sequence, Bull. Earthq. Eng. 17 (2019) 5609–5629, https://doi.org/10.1007/s10518-018-0448-z.
[65] Y. Saretta, L. Sbrogiò, M.R. Valluzzi, Assigning the macroseismic vulnerability classes to strengthened ordinary masonry buildings: an update from extensive data of the 2016 Central Italy earthquake, Int. J. Disaster Risk Reduc. 62 (2021) 102318, https://doi.org/10.1016/j.ijdrr.2021.102318.
[66] V. Follador, P. Carpanese, M. Donà, S. Alfano, S. Cattari, S. Lagomarsino, F. Da Porto, Comparison of fragility sets to assess the effectiveness of retrofit interventions on masonry buildings in Italy, Buildings 13 (2023) 2937, https://doi.org/10.3390/buildings13122937.
[67] Y. Saretta, L. Sbrogiò, M.R. Valluzzi, Seismic response of masonry buildings in historical centres struck by the 2016 Central Italy earthquake. Calibration of a vulnerability model for strengthened conditions, Construct. Build. Mater. 299 (2021) 123911, https://doi.org/10.1016/j.conbuildmat.2021.123911.
[68] MIT, Ministry of Infrastructures and Transportations, Regulation no. 7/2019, Istruzioni per l'applicazione dell'«Aggiornamento delle "Norme tecniche per le costruzioni"» di cui al decreto ministeriale 17 gennaio 2018. (in Italian).
[69] Federal Emergency Management Agency (FEMA), Rapid visual screening of buildings for potential seismic hazards: a handbook (FEMA P-154), Washington DC, USA, https://doi.org/10.4231/D3M90238V, 2015.
[70] B. Calderoni, E.A. Cordasco, M. Del Zoppo, A. Prota, Damage assessment of modern masonry buildings after the L'Aquila earthquake, Bull. Earthq. Eng. 18 (2020) 2275–2301, https://doi.org/10.1007/s10518-020-00784-5.
[71] L. Sbrogiò, Y. Saretta, M.R. Valluzzi, Empirical performance levels of strengthened masonry buildings struck by the 2016 Central Italy earthquake: proposal of a new taxonomy, Int. J. Architect. Herit. 17 (2023) 1017–1042, https://doi.org/10.1080/15583058.2021.2011474.
[72] FVG, Regione autonoma del Friuli-Venezia Giulia, Legge Regionale n. 30, 20 giugno 1977, Documento Tecnico, novembre 1977/n. 2, Raccomandazioni per la riparazione strutturale degli edifici in muratura.
[73] R. Sisti, M. Di Ludovico, A. Borri, A. Prota, Seismic performance of strengthened masonry structures: actual behaviour of buildings in Norcia and Campi Alto during the 2016 Central Italy seismic sequence, Bull. Earthq. Eng. 20 (2022) 321–348, https://doi.org/10.1007/s10518-021-01248-0.
[74] S. Mazzoni, G. Castori, C. Galasso, P. Calvi, R. Dreyer, E. Fischer, A. Fulco, L. Sorrentino, J. Wilson, A. Penna, G. Magenes, 2016–2017 Central Italy earthquake sequence: seismic retrofit policy and effectiveness, Earthq. Spectra 34 (2018) 1671–1691, https://doi.org/10.1193/100717EQS197M.
[75] F. Doglioni, Processi di trasformazione e forme di vulnerabilità, in: D. Fiorani, D. Esposito (Eds.), Tecniche Costruttive Dell'edilizia Storica: Conoscere Per Conservare, Viella, Roma, 2005, pp. 219–231.
[76] A. Giuffrè (Ed.), Sicurezza e conservazione dei centri storici. Il caso Ortigia, Laterza, Roma-Bari, 1993.
[77] A. Rovida, M. Locati, R. Camassi, B. Lolli, P. Gasperini, A. Antonucci, Catalogo Parametrico dei Terremoti Italiani (CPTI15), versione 4.0. https://doi.org/10.13127/CPTI/CPTI15.4, 2022.
[78] A. Rovida, A. Rovida, M. Locati, A. Antonucci, R. Camassi, Archivio storico macrosismico italiano (ASMI). https://doi.org/10.13127/ASMI, 2017.
[79] M. Locati, R. Camassi, A. Rovida, E. Ercolani, F. Bernardini, V. Castelli, C.H. Caracciolo, A. Tertulliani, A. Rossi, R. Azzaro, S. D'Amico, A. Antonucci, Database macrosismico italiano (DBMI15), versione 4.0, 3229 earthquakes, https://doi.org/10.13127/DBMI/DBMI15.4, 2022.

[80] L. Graziani, S. del Mese, A. Tertulliani, L. Arcoraci, A. Maramai, A. Rossi, Investigation on damage progression during the 2016–2017 seismic sequence in Central Italy using the European Macroseismic Scale (EMS-98), Bull. Earthq. Eng. 17 (2019) 5535–5558, https://doi.org/10.1007/s10518-019-00645-w.
[81] A. Rossi, A. Tertulliani, R. Azzaro, L. Graziani, A. Rovida, A. Maramai, V. Pessina, S. Hailemikael, G. Buffarini, F. Bernardini, R. Camassi, S. Del Mese, E. Ercolani, A. Fodarella, M. Locati, G. Martini, A. Paciello, S. Paolini, L. Arcoraci, C. Castellano, V. Verrubbi, M. Stucchi, The 2016–2017 earthquake sequence in Central Italy: macroseismic survey and damage scenario through the EMS-98 intensity assessment, Bull. Earthq. Eng. 17 (2019) 2407–2431, https://doi.org/10.1007/s10518-019-00556-w.
[82] M. Vettore, Y. Saretta, L. Sbrogiò, M.R. Valluzzi, A new methodology for the survey and evaluation of seismic damage and vulnerability entailed by structural interventions on masonry buildings: validation on the town of Castelsantangelo sul Nera (MC), Italy, Int. J. Architect. Herit. 16 (2022) 182–207, https://doi.org/10.1080/15583058.2020.1766159.
[83] C. Felicetta, E. Russo, M.C. D'Amico, S. Sgobba, G. Lanzano, C. Mascandola, F. Pacor, L. Luzi, Italian ACcelerometric Archive (ITACA), Version 4.0, Istituto Nazionale di Geofisica e Vulcanologia (INGV), 2023, https://doi.org/10.13127/ITACA.4.0.
[84] MIT, Ministry of Infrastructures and Transportations, Ministerial Decree 17/01/2018, Aggiornamento delle «Norme Tecniche per le costruzioni». (in Italian).
[85] MIT, Ministry of Infrastructures and Transportations, Ministerial Decree 14/01, Approvazione delle nuove Norme Tecniche per le Costruzioni, 2008 (in Italian).
[86] A. Masi, L. Chiauzzi, G. Nicodemo, V. Manfredi, Correlations between macroseismic intensity estimations and ground motion measures of seismic events, Bull. Earthq. Eng. 18 (2020) 1899–1932, https://doi.org/10.1007/s10518-019-00782-2.
[87] J.A. Nelder, R. Mead, A simplex method for function minimization, Comput. J. 7 (1965) 308–313, https://doi.org/10.1093/comjnl/7.4.308.